Stabilization of cat paw trajectory during locomotion

Alexander N. Klishko, Bradley J. Farrell, Irina N. Beloozerova, Mark L. Latash and Boris I. Prilutsky

J Neurophysiol 112:1376-1391, 2014. First published 3 June 2014; doi:10.1152/jn.00663.2013

Journal of Neurophysiology publishes original articles on the function of the nervous system. It is published 12 times a year (monthly) by the American Physiological Society, 9650 Rockville Pike, Bethesda MD 20814-3991. ISSN: 0022-3077, ESSN: 1522-1598. Visit our website at http://www.the-aps.org/.

J Neurophysiol 112: 1376–1391, 2014.
First published June 4, 2014; doi:10.1152/jn.00663.2013.

Stabilization of cat paw trajectory during locomotion

Alexander N. Klishko,[1] Bradley J. Farrell,[1] Irina N. Beloozerova,[2] Mark L. Latash,[3] and Boris I. Prilutsky[1]

[1]*School of Applied Physiology, Center for Human Movement Studies, Georgia Institute of Technology, Atlanta, Georgia;* [2]*Barrow Neurological Institute, St. Joseph's Hospital and Medical Center, Phoenix, Arizona; and* [3]*Department of Kinesiology, Penn State University, University Park, Pennsylvania*

Submitted 15 September 2013; accepted in final form 3 June 2014

Klishko AN, Farrell BJ, Beloozerova IN, Latash ML, Prilutsky BI. Stabilization of cat paw trajectory during locomotion. *J Neurophysiol* 112: 1376–1391, 2014. First published June 4, 2014; doi:10.1152/jn.00663.2013.—We investigated which of cat limb kinematic variables during swing of regular walking and accurate stepping along a horizontal ladder are stabilized by coordinated changes of limb segment angles. Three hypotheses were tested: *1*) animals stabilize the entire swing trajectory of specific kinematic variables (performance variables); and *2*) the level of trajectory stabilization is similar between regular and ladder walking and *3*) is higher for forelimbs compared with hindlimbs. We used the framework of the uncontrolled manifold (UCM) hypothesis to quantify the structure of variance of limb kinematics in the limb segment orientation space across steps. Two components of variance were quantified for each potential performance variable, one of which affected it ("bad variance," variance orthogonal to the UCM, V_{ORT}) while the other one did not ("good variance," variance within the UCM, V_{UCM}). The analysis of five candidate performance variables revealed that cats during both locomotor behaviors stabilize *1*) paw vertical position during the entire swing ($V_{UCM} > V_{ORT}$, except in mid-hindpaw swing of ladder walking) and *2*) horizontal paw position in initial and terminal swing (except for the entire forepaw swing of regular walking). We also found that the limb length was typically stabilized in midswing, whereas limb orientation was not ($V_{UCM} \leq V_{ORT}$) for both limbs and behaviors during entire swing. We conclude that stabilization of paw position in early and terminal swing enables accurate and stable locomotion, while stabilization of vertical paw position in midswing helps paw clearance. This study is the first to demonstrate the applicability of the UCM-based analysis to nonhuman movement.

uncontrolled manifold analysis; principle of abundance; walking; accurate stepping; cat

ONE OF THE CENTRAL PROBLEMS of motor control is the problem of motor redundancy (Bernstein 1967). It reflects the fact that, in any analysis of the neuromotor system, the number of elemental variables (those produced by system's elements, i.e., body limbs, joints, muscles, etc.) is higher than the number of constraints associated with typical motor tasks. For example, the same movement of the hand or foot can be performed with different combinations of joint angles of the limb because the number of degrees of freedom (DOF) in the upper and lower extremities exceeds the number of space dimensions [two- (2D) or three-dimensional (3D)] in which the endpoint of the limb is constrained to move. Given an unlimited choice of combinations of elemental variables (e.g., joint angles) to move the limb endpoint along a trajectory, how does the nervous system select specific combinations of elemental variables to organize the movement? Recently, an approach to solving this problem has been developed based on the principle of abundance (Gelfand and Latash 1998; Latash 2012). According to this principle, the central nervous system (CNS) often does not look for single optimal solutions to problems of motor redundancy, but facilitates families of solutions equally capable of solving the task. A signature of this control strategy is a particular pattern of variance in the space of elemental variables. A quantitative method for analysis of motor variance has been developed within the uncontrolled manifold (UCM) hypothesis (Latash et al. 2007; Scholz and Schoner 1999). Within this method, variance across consecutive trials or cycles (for a cyclic task) is partitioned into two components. One of them (variance within the UCM, V_{UCM} or "good variability") keeps a potentially important performance variable unchanged, while the other (variance orthogonal to the UCM, V_{ORT} or "bad variability") leads to changes in that variable. Neural mechanisms responsible for variance distributions characterized by an inequality $V_{UCM} > V_{ORT}$ have been referred to as "synergies."

The term "synergy" has been used in the literature in at least three meanings. In clinical literature, this word has a strong negative connotation and implies pathological, stereotypical patterns of muscle activation (e.g., after stroke) interfering with voluntary movements (Bobath 1978; Dewald et al. 1995). In a more traditional meaning, synergy means a group of variables that scale together during changes in task parameters and/or over time; methods of matrix factorization have been commonly used to identify such groups of variables (reviewed in Ting and McKay 2007). This definition follows the traditions set by Bernstein (1967), who viewed such grouping as a method of reducing the number of variables a hypothetical neural controller has to manipulate. Our definition links the notion of synergies to stability of movements, which is paramount for successful performance in the changing environment.

There is no agreed-upon hypothesis on the origin of motor synergies (in our definition). Synergies have been described as products of an optimal feedback control scheme, a feedforward scheme, a scheme with central back-coupling loops, and a hierarchical scheme based on ideas of equilibrium-point control (Goodman and Latash 2006; Latash 2010; Latash et al. 2005; Martin et al. 2009; Todorov and Jordan 2002). Most of these schemes make no claims regarding potential roles of different brain regions in synergies. Studies of patients with cortical and subcortical disorders (Park et al. 2012, 2013; Reisman and Scholz 2003) point at subcortical loops, possibly

Address for reprint requests and other correspondence: Boris I. Prilutsky, School of Applied Physiology, Georgia Institute of Technology, 555 14th St. NW, Atlanta, Georgia 30332-0356 (e-mail: boris.prilutsky@ap.gatech.edu).

those involving the basal ganglia and the cerebellum, as crucial for synergy formation in humans.

As of now, all of the experimental evidence in favor of the principle of abundance and the idea of synergies has come from studies on people. A number of studies of animals, including reduced animal preparations, suggest that synergies may be organized at the spinal cord level (Berkinblit et al. 1986; Boyce and Lemay 2009; Hultborn et al. 2004; Mussa-Ivaldi et al. 1994). However, only indirect animal studies of the structure of variance have been available (Bauman and Chang 2013; Chang et al. 2009). One of the main goals of the current study has been to provide evidence for synergies stabilizing potentially important performance variables during a natural behavior of intact cats. We selected locomotion as the behavior of interest because, first, the central role of the spinal cord in the production of locomotion has been well established; second, one can formulate reasonable hypotheses with respect to kinematic performance variables that may be stabilized by a multijoint synergy; and third, comparing synergies in the forelimbs and hindlimbs allows the exploration of the potential role of vision in such synergies.

It is well known that animals, including humans, can voluntarily modify the location of foot placement during locomotion when they step on specific support surfaces (Beloozerova and Sirota 1993a, 1993b; Metz and Whishaw 2002), circumvent or step over obstacles (Lavoie et al. 1995; Patla and Greig 2006), walk along a prescribed path (Galvez-Lopez et al. 2011; McAndrew Young et al. 2012), or alter stride length and stance width when stability of locomotion is threatened (Dingwell et al. 2008; MacLellan and Patla 2006; Marigold and Patla 2008). Potentially, several motor strategies are available to provide accurate foot placement to a selected location. An entire foot trajectory could be planned before initiation of swing (Hollands and Marple-Horvat 1996, 2001) to enable safe foot clearance over the ground, and any deviation from the trajectory is corrected. Alternatively, foot trajectory could be stabilized only in the vicinity of a foot placement location (Reynolds and Day 2005) or in early swing of locomotion.

During quadrupedal locomotion, the animal can see only the final part of forepaw trajectory prior to paw contact with the ground, whereas the initial part of the forepaw trajectory and the entire hindpaw trajectory cannot be seen. Nevertheless, displacements and symmetric bell-shaped velocity profiles of fore- and hindpaws look essentially identical during swing of regular walking and skilled accurate stepping on a horizontal ladder (Beloozerova et al. 2010; Prilutsky et al. 2005), suggesting that, in these tasks, paw placements are planned in advance and are not corrected during swing (Beloozerova et al. 2010). Alternatively, a stereotypic paw trajectory of each limb during swing could result from a continuous or intermittent stabilization of limb endpoint position by coordinated small changes in joint angles such that they reduce variability of the paw based on a combination of visual and proprioceptive feedback. This stabilization of paw trajectory could potentially explain substantial changes in the modulation of neural activity from limbs' representation in the motor cortex during swing of skilled accurate stepping compared with the activity of the same cortical cells during regular walking, despite virtually identical limb kinematics (Beloozerova et al. 2010).

We approached the analysis of multijoint synergies potentially stabilizing the paw trajectory or other limb kinematic variables using the method developed within the UCM hypothesis. Namely, for each time sample of the swing phase, V_{UCM} and V_{ORT} were computed across consecutive strides, both quantified per DOF in the corresponding spaces, and then a "synergy index" (ΔV) was computed reflecting the relative difference between V_{UCM} and V_{ORT}. $V_{UCM} > V_{ORT}$ ($\Delta V > 0$) is interpreted as a reflection of a purposeful neural strategy stabilizing the performance variable. In some motor behaviors, like blacksmith hammering (Bernstein 1923) or pistol shooting (Scholz et al. 2000), the performance variables can be reasonably assumed a priori, and their stabilization tested using the UCM analysis. In locomotor behaviors, hypothetical performance variables are not obvious, and their selection for the UCM analysis requires careful considerations.

During skilled walking on a horizontal ladder, i.e., accurate stepping, the cat walks by placing paws on 5-cm-wide crosspieces of the ladder (Beloozerova et al. 2010; Beloozerova and Sirota 1993a). This locomotor behavior is trained for about 1 mo using operant conditioning and food rewards (see METHODS), and once the task is learned the cat never fails to place paws on the ladder crosspieces during walking. Thus in this locomotor behavior, paw position during swing can be hypothesized to be a performance variable. Recent studies on dynamic stability of regular walking in humans (Hof et al. 2005, 2007) and cats (Farrell et al. 2014) have also demonstrated the importance of accurate foot or paw placement in front of the extrapolated center of mass of the body to maintain dynamic stability in the frontal and sagittal planes. Therefore, it is reasonable to assume that paw position during cat regular walking could be a performance variable. Other potential performance variables during cat regular walking that appear to be stabilized by multijoint kinematic synergies even after injury of major ankle extensors are the limb length and orientation (Bauman and Chang 2013; Chang et al. 2009), whose values may be encoded in the activity of the dorsal spinocerebellar tract neurons (Bosco et al. 2000).

Our more specific hypotheses related to possible differences in stabilization of the potential fore- and hindlimb performance variables during swing and between regular walking and accurate stepping on crosspieces of a horizontal ladder. Three hypotheses were tested: *1*) animals stabilize the entire trajectory of the performance variable during swing [based on human studies (Domkin et al. 2005; Krishnan et al. 2013)]; *2*) the index of performance variable trajectory stabilization during walking on a horizontal ladder is similar to that during regular walking [based on studies showing no correlation between indexes of stabilization and accuracy of performance (Gorniak et al. 2008; Shapkova et al. 2008)]; and *3*) the index of performance variable trajectory stabilization is higher for forepaws compared with hindpaws [based on the importance of visual information for accurate stepping (Marigold and Patla 2008; Reynolds and Day 2005)].

METHODS

Subjects and Experimental Procedures

Locomotor kinematics of hind- and forelimbs were obtained from recordings of five adult cats (3 males and 2 females), participants of a larger study; animal characteristics are shown in Table 1. All experimental procedures were conducted in accordance with the US Public Health Service Policy on Humane Care and Use of Laboratory Animals and with

Table 1. *Individual and mean cat characteristics*

Parameter	Cat					Mean ± SD
	BU	BL	AG	C8	FM	
Upper arm length, mm	93	88	110	103	103	99 ± 9
Forearm length, mm	93	89	125	113	110	106 ± 15
Carpals + digits length, mm	35	36	35	40	30	35 ± 4
Thigh length, mm	98	100	110	110	105	105 ± 6
Shank length, mm	98	100	115	133	116	112 ± 14
Tarsals + digits length, mm	72	78	75	68	67	72 ± 5
Mass, kg	3.1	3.0	4.6	4.5	4.0	3.8 ± 0.8

the approval of the Institutional Animal Care and Use Committees of both Georgia Institute of Technology and Barrow Neurological Institute.

Cats were trained for at least 1 mo to walk along a walkway in a Plexiglas-enclosed chamber on a flat surface and on a horizontal ladder (crosspieces 5 cm wide) using food reward (for details see Beloozerova et al. 2010; Gregor et al. 2006; Prilutsky et al. 2005). Food reward, several dry food pellets, was given each time the cat walked across the walkway with or without horizontal ladder with a steady speed. The cat consumed pellets during short breaks of 5–15 s before initiating the next walking trial and continued walking until it lost interest in food and stopped eating after completing 50–80 trials. After training, high-speed (sampling frequency 112–120 Hz) motion capture systems Vicon (Vicon Motion Systems) or Visualeyez System (Phoenix Technologies) were used to record 3D coordinates of markers attached to shaved skin over bony landmarks of the cat body using double-sided adhesive tape (Fig. 1) (Beloozerova et al. 2010; Prilutsky et al. 2005). Marker locations used in this study included the greater trochanter (hip joint), approximate knee joint center, lateral malleolus (ankle joint), base of the fifth metatarsal (metatarsophalangeal joint) of one or both hindlimbs and the greater tubercle (shoulder joint), approximate elbow joint center, ulna styloid process (wrist joint), base of the fifth metacarpal (metacarpophalangeal joint) of one or both forelimbs. The animals performed regular walking and accurate stepping within one experimental session, either intermittently by continuously crossing interconnected walkways with flat surface and a horizontal ladder or sequentially by performing multiple trials of one locomotion task before switching to the other task; the order of tasks was balanced between cats. The distance between crosspieces of the horizontal ladder was set for each cat to be approximately equal to the mean cat's step length of regular walking with self-selected speed (on average, about 25 cm).

Length of each segment of the fore- and hindlimb (Table 1) was measured using a caliper while the animal was sedated (dexmedetomidine, 40–60 μg/kg sc).

Data Processing

All recorded walking trials were screened to ensure that only cycles in which cats walked with a constant, steady speed were used for further analysis. Recorded marker displacement data of the main joints of left and/or right fore- and hindlimbs (Fig. 1) in the sagittal plane were low-pass filtered (fourth-order, zero-phase lag Butterworth filter, 10-Hz cutoff frequency). To minimize displacement errors caused by skin motion near the knee and elbow joints (Miller et al. 1975), coordinates of these joints were recalculated using recorded joint marker positions of the adjacent joints and measured length of the segments forming the knee and elbow joints. For example, for each instant of time, the position of the knee joint center in the sagittal plane was determined trigonometrically as an intersection point between the two circles with the centers located at the ankle joint marker and the hip joint marker positions and with the circles' radii corresponding to the shank length and thigh length, respectively. Out of two intersection points, the one corresponding to the anatomical constraint on maximum knee extension (<180°) was selected. The same procedure was used to determine the position of the elbow joint in the sagittal plane.

The relative position of the limb endpoint with respect to the limb most proximal joint (hip or shoulder) was used to identify the swing phase onset (paw-off, PO) and offset (paw contact, PC), as described elsewhere (Pantall et al. 2012). Each analyzed stride cycle was defined as the period between consecutive PO instances; the swing phase was defined as the period between PO and PC. The smoothed marker displacements were time normalized within each walking cycle and swing phase.

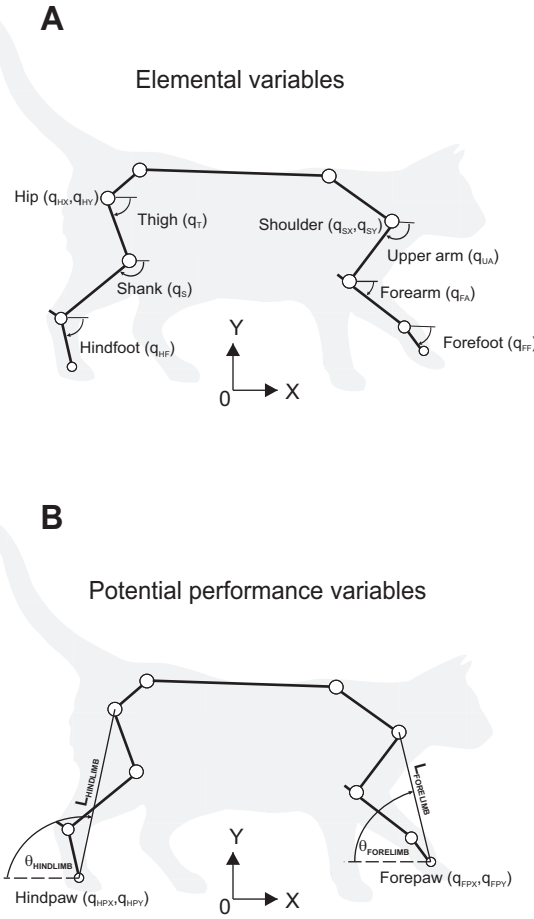

Fig. 1. Kinematic model of fore- and hindlimbs used for uncontrolled manifold (UCM) analysis. *A*: kinematics of each limb is described by 5 generalized coordinates (elemental variables): Cartesian *x*- and *y*-coordinates of suspension point [hip (H) or shoulder (S)] and 3 segment angles with the horizon [thigh (T) or upper arm (UA), shank (S) or forearm (FA), hindfoot (HF) or forefoot (FF)] (hindfoot comprises tarsals and hind digits, forefoot consists of carpals and fore digits). *B*: potential performance variables for UCM analysis are the two-dimensional (2D) position of the limb endpoint, i.e., Cartesian *x*- and *y*-coordinates of forepaw (FP) or hindpaw (HP), vertical or horizontal position of the paw, limb length (L) and limb orientation (θ). The open circles indicate positions of reflective markers for motion capture.

A 2D, 5 DOF kinematic model of a limb was used to describe kinematics of the fore- and hindlimb (Fig. 1) and derive the Jacobian matrix (see below). Generalized coordinates describing model kinematics included the Cartesian horizontal and vertical coordinates of the limb suspension point (the hip joint for hindlimb and the shoulder joint for forelimb) and three segment angles with respect to the horizon (Fig. 1: thigh, shank, and foot angles for the hindlimb and upper arm, forearm and fore foot angles for the forelimb). Since UCM analysis, as described in the Introduction, involves calculations of variance of kinematic variables at the same normalized time instant across walking cycles, it is important to ensure that each elemental kinematic variable has a similar periodic pattern within walking cycles. All generalized coordinates of the limb model are periodic functions of walking cycle time, except for the horizontal displacement of the hip and shoulder joints (e.g., Prilutsky et al. 2005). To make these latter variables periodic, a linear trend (a linear regression between the horizontal joint displacement and normalized cycle time) was computed and then subtracted from the horizontal displacement of the joint at each percent of the cycle time. This detrending procedure is analogous to determining horizontal coordinates of a joint in a coordinate frame moving with a constant speed corresponding to the average speed of walking in a given cycle. In other words, the obtained detrended horizontal coordinates of the hip and shoulder can be considered displacements, as observed during walking on a treadmill operating at a constant speed.

Uncontrolled Manifold Analysis

We used the framework of the UCM analysis (Latash et al. 2007; Scholz et al. 2000; Scholz and Schoner 1999) to partition variance of elemental kinematic task variables (limb generalized coordinates) at each time instant across multiple walking cycles into two subspaces. One subspace (UCM) consists of variance of elemental variables that does not affect a performance variable, V_{UCM} ("good variance"); the second subspace is orthogonal to the first one and contains variance that affects a performance variable, V_{ORT} ("bad variance"). Both variance components, V_{UCM} and V_{ORT}, were computed for each instance of the normalized walking cycle time and then normalized per DOF of the corresponding subspace. To examine whether a performance variable was stabilized over walking cycles by coordinated changes in elemental variables, the V_{UCM} and V_{ORT} were compared by analyzing their normalized difference (index of synergy, ΔV, e.g., Klous et al. 2011).

Potential performance and elemental variables. As discussed in the Introduction, five limb kinematic variables could be assumed to be stabilized by multijoint kinematic synergies during swing of regular and ladder walking: *1*) 2D paw position in the global coordinate frame related to the ground; *2*) horizontal paw position in the global coordinate frame; *3*) vertical paw position in the global coordinate frame; *4*) limb length (the distance between the most proximal joint and the paw); and *5*) limb orientation.

To examine stabilization of potential performance *variable 1*, 2D paw position, the global Cartesian horizontal x and vertical y coordinates of the paw were expressed as functions of five elemental task variables (generalized limb coordinates; Fig. 1):

$$\begin{cases} x = q_1 + L_3 \cos q_3 + L_4 \cos q_4 + L_5 \cos q_5 \\ y = q_2 - L_3 \sin q_3 - L_4 \sin q_4 - L_5 \sin q_5 \end{cases} \quad (1)$$

where generalized limb coordinates are as follows: q_1 and q_2, horizontal and vertical coordinates of hip (shoulder) joint; q_3, q_4 and q_5, angles formed by the thigh (upper arm), shank (forearm), and tarsals (carpals) with the horizon; L_3, L_4, L_5, lengths of the thigh (upper arm), shank (forearm), and tarsals (carpals), respectively (Table 1). In contrast to some previous UCM analyses (Auyang et al. 2009; Kapur et al. 2010; Latash et al. 2007; Scholz and Schoner 1999), we used heterogeneous elemental variables with different dimensions, i.e., angles and Cartesian linear coordinates, to analyze stabilization of paw 2D position or paw's vertical and horizontal positions separately. Note that similar approaches were used earlier (e.g., Yang and Scholz 2005). To eliminate dependence of computed variance of elemental variables on their dimensions, the variables were substituted by new variables using the range of variables' changes (R_i) across analyzed cycles ($R_i = q_i^{max} - q_i^{min}$, $i = 1, \ldots, 5$; where q_i^{max} and q_i^{min} are maximum and minimum values, respectively, of ith elemental variable across walking cycles for a given cat and limb, Table 2). For horizontal coordinate q_1, the range was determined after the detrending procedure. By introducing new elemental variables $\hat{q}_i = (q_i - q_i^{min})/R_i$ that change between 0 and 1, system (*Eq. 1*) can be rewritten as:

$$\begin{cases} x = (q_1^{min} + R_1\hat{q}_1) + L_3 \cos(q_3^{min} + R_3\hat{q}_3) + L_4 \cos(q_4^{min} + R_4\hat{q}_4) + L_5 \cos(q_5^{min} + R_5\hat{q}_5) \\ y = (q_2^{min} + R_2\hat{q}_2) - L_3 \sin(q_3^{min} + R_3\hat{q}_3) - L_4 \sin(q_4^{min} + R_4\hat{q}_4) - L_5 \sin(q_5^{min} + R_5\hat{q}_5) \end{cases} \quad (1a)$$

The Jacobian of system (*Eq. 1a*) for each time instant is

$$\boldsymbol{J}_{x,y} = \begin{bmatrix} R_1 & 0 & -L_3R_3 \sin q_3 - L_4R_4 \sin q_4 - L_5R_5 \sin q_5 \\ 0 & R_2 & -L_3R_3 \cos q_3 - L_4R_4 \cos q_4 - L_5R_5 \cos q_5 \end{bmatrix} \quad (2)$$

The Jacobian $\mathbf{J}_{x,y}$ was used for computing the V_{UCM} and V_{ORT} of the five elemental variables describing the 2D paw position (see below).

The Jacobians $\mathbf{J}_x$ and $\mathbf{J}_y$ for computing V_{UCM} and V_{ORT} for paw horizontal and vertical positions (potential performance *variables 2* and *3*) in the space of the same five elemental variables corresponded to the first and second rows of matrix (2).

The Jacobian $\mathbf{J}_L$ for computing V_{UCM} and V_{ORT} for limb length (potential performance *variable 4*) in the space of three limb segment angles q_3, q_4, and q_5 (Fig. 1) is:

$$\boldsymbol{J}_L = [-\frac{L_3}{L}(x_L \sin q_3 + y_L \cos q_3) - \frac{L_4}{L}(x_L \sin q_4 + y_L \cos q_4) - \frac{L_5}{L}(x_L \sin q_5 + y_L \cos q_5)] \quad (2a)$$

where L_3, L_4, and L_5 are lengths of three limb segments in the fore- or hindlimb (Fig. 1); $L = \sqrt{x_L^2 + y_L^2}$ is the fore- or hindlimb length; $x_L =$

Table 2. *Ranges of elemental variables describing paw position in the global coordinate system for fore- and hindlimbs during locomotor tasks*

Cat	Limb	R_{q1}, mm	R_{q2}, mm	R_{q3}, °	R_{q4}, °	R_{q5}, °
AG	Fore	63	47	81	85	125
	Hind	61	70	77	79	112
BL	Fore	75	37	84	117	137
	Hind	55	41	96	91	96
BU	Fore	81	45	104	108	152
	Hind	42	53	98	92	95
C8	Fore	72	63	95	118	169
	Hind	62	57	77	63	109
FM	Fore	73	60	73	113	106
	Hind	44	45	69	76	84

$L_3 \cos q_3 + L_4 \cos q_4 + L_5 \cos q_5$ is the horizontal hind- or forepaw coordinate with respect to the hip or shoulder joint; $y_L = -(L_3 \sin q_3 + L_4 \sin q_4 + L_5 \sin q_5)$ is the vertical hind- or forepaw coordinate with respect to the hip or shoulder joint.

The Jacobian $\mathbf{J}_\theta$ for computing V_{UCM} and V_{ORT} for limb orientation (potential performance *variable 5*) in the space of three limb segment angles q_3, q_4, and q_5 (Fig. 1) is:

$$\boldsymbol{J}_\theta = [-L_3(y_L \sin q_3 - x_L \cos q_3) - L_4(y_L \sin q_4 - x_L \cos q_4) - L_5(y_L \sin q_5 - x_L \cos q_5)] \quad (2b)$$

For each potential performance variable, the corresponding Jacobian was used to linearize limb forward kinematics in the vicinity of the limb reference configuration at each time instant of *j*th walking cycle (Scholz and Schoner 1999):

$$\boldsymbol{r}_j - \bar{\boldsymbol{r}} = \boldsymbol{J}_j(\boldsymbol{q}_j - \bar{\boldsymbol{q}}) \quad (3)$$

where $\mathbf{r_j}$ and $\mathbf{q_j}$ are vectors of performance variable components and elemental variables in cycle *j* and $\bar{\mathbf{r}}$ and $\bar{\mathbf{q}}$ are vectors of performance and elemental variables in the limb reference configuration, respectively; the reference limb configuration was set for each normalized cycle time instant as the mean limb configuration across all walking cycles within the task and animal (Figs. 2 and 3). For each time instant, the projection of deviations of the limb segment configuration vector from the limb reference configuration vector ($\Delta\mathbf{q}_j = \mathbf{q}_j - \bar{\mathbf{q}}$) onto the Jacobian's null-space is computed as:

$$\Delta\boldsymbol{q}_{\|j} = \sum_{i=1}^{3} \boldsymbol{e}_i \Delta\boldsymbol{q}_j \quad (4)$$

whereas the component of limb configuration deviations perpendicular to the null-space is

$$\Delta\boldsymbol{q}_{\perp j} = \Delta\boldsymbol{q}_j - \Delta\boldsymbol{q}_{\|j} \quad (5)$$

where the basis vector **e** defines the null-space of the Jacobian ($0 = \mathbf{Je}$), for which deviations of limb segment configurations in the vicinity of the reference limb configuration do not affect paw position. The amount of variance per DOF within the UCM (good variance) is

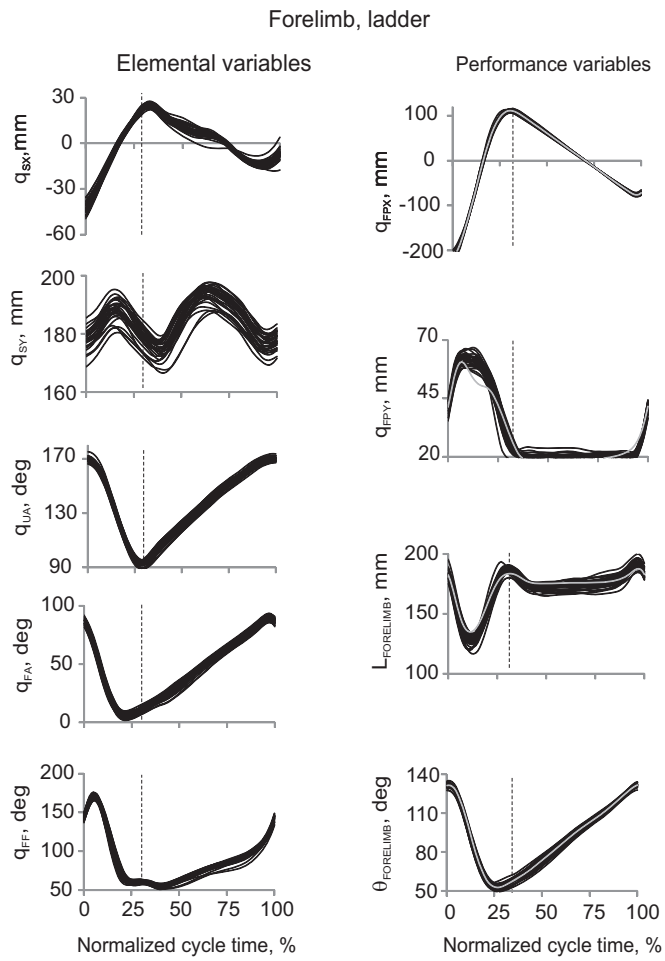

Fig. 2. Examples of forelimb elemental (*left*) and potential performance variables (*right*) during 30 cycles of ladder walking from a representative cat BL. Each individual cycle is represented by a thin black line. Vertical dashed line in each panel separates the swing and stance phase. *Left* (from *top* to *bottom*): Cartesian horizontal q_{SX} (after detrending, see text) and vertical q_{SY} coordinates of the shoulder, orientation angles of the upper arm q_{UA}, forearm q_{FA} and forefoot q_{FF} (for definition of the elemental variables, see Fig. 1). *Right* (from *top* to *bottom*): Cartesian horizontal q_{FPX} (after detrending) and vertical q_{FPY} coordinates of the forepaw, forelimb length $L_{FORELIMB}$ and forelimb orientation $\theta_{FORELIMB}$ (for definition of the potential performance variables see Fig. 1). The gray line in each panel represents the mean of the linearized forward kinematics solutions computed for 30 walking cycles (see *Eq. 3*).

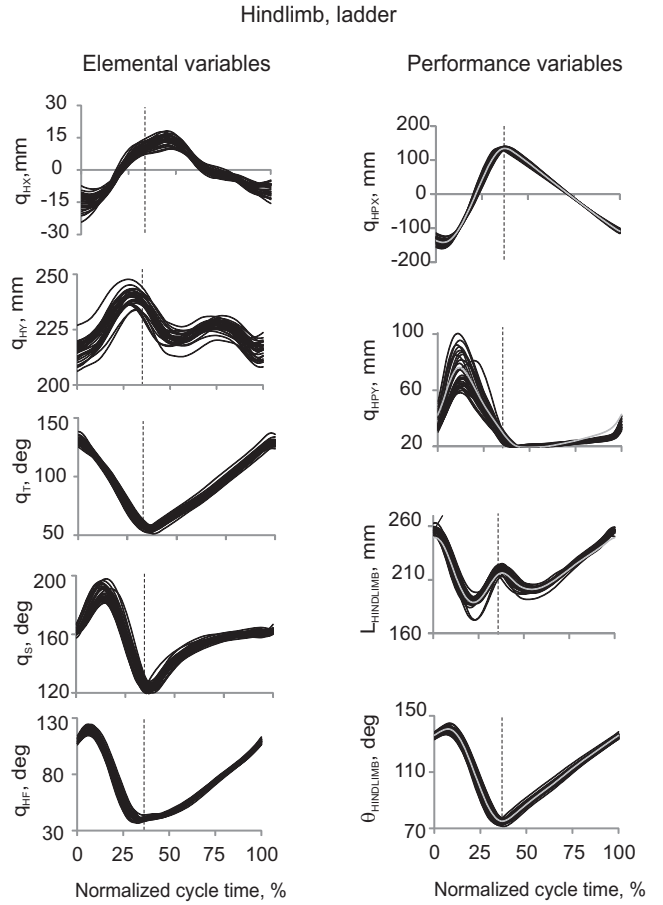

Fig. 3. Examples of hindlimb elemental (*left*) and potential performance variables (*right*) during 30 cycles of ladder walking from a representative cat BL. Each individual cycle is represented by a thin black line. Vertical dashed line in each panel separates the swing and stance phase. *Left* (from *top* to *bottom*): Cartesian horizontal q_{HX} (after detrending, see text) and vertical q_{HY} coordinates of the hip, orientation angles of the thigh q_T, shank q_S and hindfoot q_{HF} (for definition of the elemental variables, see Fig. 1). *Right* (from *top* to *bottom*): Cartesian horizontal q_{HPX} (after detrending) and vertical q_{HPY} coordinates of the hindpaw, hindlimb length $L_{HINDLIMB}$ and hindlimb orientation $\theta_{HINDLIMB}$ (for definition of the potential performance variables, see Fig. 1). The gray line in each panel represents the mean of the linearized forward kinematics solutions computed for 30 walking cycles (see *Eq. 3*).

$$V_{UCM} = \frac{1}{N_{UCM}(N-1)} \sum_{j=1}^{N} \Delta q_{\|j}^2 \quad (6)$$

where N is the number of cycles and N_{UCM} is the dimension of the UCM. The amount of variance per DOF in the space orthogonal to the null-space (bad variance) is

$$V_{ORT} = \frac{1}{N_{ORT}(N-1)} \sum_{j=1}^{N} \Delta q_{\perp j}^2 \quad (7)$$

where N_{ORT} is the number of DOF for the space orthogonal to the UCM. The amount of total variance per DOF is

$$V_{TOT} = \frac{1}{N_{TOT}(N-1)} \sum_{j=1}^{N} \Delta q_j^2 \quad (8)$$

where N_{TOT} is the number of DOF of the elemental variables.

The index of synergy ΔV was computed as

$$\Delta V = (V_{UCM} - V_{ORT})/V_{TOT} \quad (9)$$

The range of ΔV changes depends on the dimensions of V_{UCM}, V_{ORT} and V_{TOT} spaces that in turn depend on dimensions of the performance variable and the number of elemental variables. It follows from *Eqs. 6–9* that values of ΔV for 2D paw position (potential performance *variable 1*) and five elemental variables (see above) can change between -2.50 and 1.67 ($N_{UCM} = 3$, $N_{ORT} = 2$, $N_{TOT} = 5$). For one-dimensional potential performance *variables 2* and *3* (horizontal and vertical paw positions analyzed separately) and the same five elemental variables, ΔV can change between -5 and 1.25 ($N_{UCM} = 4$, $N_{ORT} = 1$, $N_{TOT} = 5$). For one-dimensional potential performance *variables 4* and *5* (limb length and limb orientation) and three elemental variables of segment angles, ΔV can change between -3 and 1.5 ($N_{UCM} = 2$, $N_{ORT} = 1$, $N_{TOT} = 3$). ΔV values higher than zero at a given time instant indicate that the potential performance variable (e.g., paw position or limb length) is stabilized by covarying across cycles elemental variable changes at this time instant.

The ΔV, ΔV_{UCM} and ΔV_{ORT} were computed for every percentage of the normalized swing phase time of each walking task and limb for each cat and potential performance variable.

Statistics

To test the effects of locomotion task, limb and swing time on the ΔV, V_{UCM} and V_{ORT}, a three-way 2 (task: regular walking, ladder walking) by 2 (limb: forelimb, hindlimb) by 10 (time: 10% time bins of swing) repeated-measures ANOVA was performed for each dependent variable. Since absolute values of ΔV are constrained by a minimum and maximum value as described above, leading to a reduction of the ΔV variance when ΔV values approach their limits, the Fisher z transformation of ΔV was performed prior to ANOVA analysis. When ANOVA analysis indicated significant results, post hoc comparisons were performed with the Bonferroni test. To test whether ΔV was significantly different from zero and if V_{UCM} and V_{ORT} were different from each other, the nonparametric Wilcoxon matched-pairs test was used. Statistical analysis was performed using software STATISTICA 7 (StatSoft, Tulsa, OK). Significance level was set at 0.05.

RESULTS

General Kinematic Characteristics of Regular and Ladder Walking

The number of analyzed walking cycles per cat, limb and walking condition was 30. Walking speed, determined as the ratio of the horizontal displacement of the limb suspension point (hip or shoulder) over the cycle time, was not statistically different among the combinations of locomotor tasks and limbs; speed ranged from 0.71 ± 0.17 m/s for hindlimb cycles of ladder walking to 0.76 ± 0.22 m/s for forelimb cycles of ladder walking (repeated-measures ANOVA, $F_{1,4} = 0.07–0.83$, $P = 0.414–0.802$, Table 3). Cycle times for different walking tasks and limbs were found to be between 685 ± 151 ms (forelimb, ladder walking) and 710 ± 37 ms (hindlimb, regular walking), and no significant difference in cycle time was detected among tasks and limbs (repeated-measures ANOVA, $F_{1,4} = 0.16–0.23$, $P = 0.66–0.71$). Forelimb swing times were 253 ± 18 ms and 247 ± 40 ms for regular and ladder walking, respectively, whereas the corresponding hindlimb swing durations were longer, 285 ± 5 ms and 277 ± 47 ms (repeated-measures ANOVA, $F_{1,4} = 229.4$, $P < 0.05$, Table 3). Duty factor (the ratio of stance time and cycle time) was accordingly lower for hindlimbs with the values of 0.60 ± 0.02 for regular and ladder walking than for forelimbs during regular and ladder walking: 0.64 ± 0.04 ms and 0.63 ± 0.03 ms, respectively (repeated-measures ANOVA, $F_{1,4} = 15.25$, $P < 0.05$). Thus general timing characteristics of fore- and hindlimb movements during regular and ladder walking were in agreement with previously published data on cat locomotion (Beloozerova et al. 2010; Miller et al. 1975; Prilutsky et al. 2005).

All cats demonstrated highly stereotypic kinematic patterns of the elemental variables: vertical and detrended horizontal coordinates of the shoulder and hip joints, fore- and hindlimb segmental angles (Figs. 2 and 3, *left*), as well as the potential performance variables: vertical and detrended horizontal coordinates of the fore- and hindpaw, limb length and limb orientation (Figs. 2 and 3, *right*) during both regular and ladder walking. Stereotypic kinematics across walking cycles within each cat were evident from the relatively small variability of the kinematic patterns and in similarity of the temporal changes in kinematic variables, i.e., their peaks and troughs were closely aligned across cycles (Figs. 2 and 3).

Linearization of limb forward kinematics in the vicinity of the limb reference configuration performed for each potential performance variable and the corresponding set of elemental variables (*Eq. 3*) gave close approximation of experimentally recorded 2D paw position, limb segment length and orientation for ladder walking (Figs. 2 and 3, *right*, gray lines) and regular walking (not shown).

Table 3. *General kinematic characteristics of fore- and hindlimbs during regular and ladder walking*

Limb	Locomotor Task	Cycle Time, ms	Swing Time, ms	Duty Factor	Walking Speed, m/s
Forelimb	Regular	709 ± 67	253 ± 18	0.64 ± 0.04	0.72 ± 0.10
Hindlimb	Regular	710 ± 37	285 ± 5	0.60 ± 0.02	0.72 ± 0.10
Forelimb	Ladder	685 ± 151	247 ± 40	0.63 ± 0.03	0.76 ± 0.22
Hindlimb	Ladder	698 ± 124	277 ± 47	0.60 ± 0.01	0.71 ± 0.17

Values are means ± SD; $n = 5$ cats.

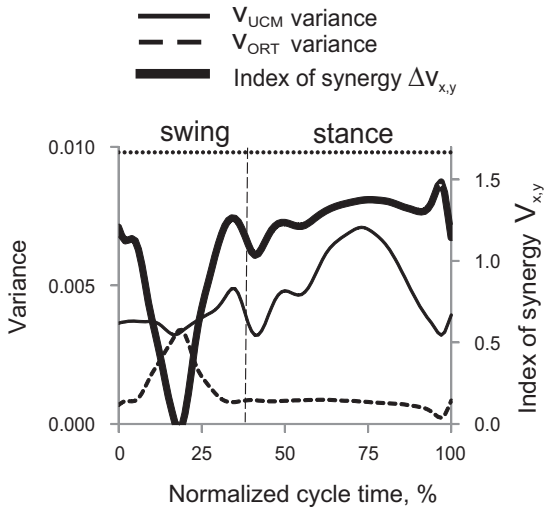

Fig. 4. Representative patterns of index of synergy ($\Delta V_{x,y}$, thick line), "good" variance (V_{UCM}, thin continuous line) and "bad" variance [variance orthogonal to the UCM (V_{ORT}), dashed line] calculated for forelimbs of one cat during a cycle of ladder walking. The left vertical axis is for V_{UCM} and V_{ORT}; the right vertical axis shows values of $\Delta V_{x,y}$. The vertical dashed line separates the swing and stance phase. The *top* horizontal dotted line indicates the theoretical maximum of $\Delta V_{x,y}$ (1.67, see text). Cat BL, ladder walking, $N = 30$.

Potential Performance Variables

2D paw position in 5D space of elemental variables. Patterns of good variance of limb kinematics ($V_{UCM_{x,y}}$), bad variance ($V_{ORT_{x,y}}$), and synergy index ($\Delta V_{x,y}$) were similar between regular and ladder walking (see a representative example for forelimbs of ladder walking in Fig. 4): V_{UCM} achieved its maximum values in midstance, V_{ORT} had one peak in midswing and values close to zero in stance, whereas $\Delta V_{x,y}$ had high positive values in early and late swing and during most of stance and was close to zero in midswing. Since this study focuses on paw trajectory during swing, the stance phase will not be considered further.

Synergy index $\Delta V_{x,y}$ patterns averaged across all cats within each task and limb had positive values throughout the whole swing phase for hindlimbs during regular walking and forelimbs during ladder walking (Wilcoxon matched-pairs test, $Z = 2.02$, $n = 5$, $P < 0.05$), indicating that the 2D paw position could be stabilized throughout the swing. Index of synergy $\Delta V_{x,y}$ for forelimb during regular walking and for hindlimbs during ladder walking was different from zero only in the beginning or first half of swing and late swing [Wilcoxon matched-pairs test, $Z = 2.02$, $n = 5$, $P < 0.05$, Fig. 5, mean (black line) ± SE (gray shadow)]. Thus the 2D forepaw position during regular walking and hindpaw position during ladder walking were not stabilized in midswing. ANOVA performed on z-transformed $\Delta V_{x,y}$ values demonstrated a significant effect of swing time ($F_{9,36} = 13.7$, $P < 0.05$, Fig. 6*A*): the index of synergy $\Delta V_{x,y}$ averaged across limbs and walking conditions for each time bin was higher at the beginning and end of swing than in midswing. There was a significant time-limb interaction effect on index of synergy $\Delta V_{x,y}$ ($F_{9,36} = 7.55$; $P < 0.05$), and no significant effects of locomotion task or limb.

The obtained partition of synergy index $\Delta V_{x,y}$ into $V_{UCM_{x,y}}$ and $V_{ORT_{x,y}}$ showed that $V_{UCM_{x,y}}$ (not affecting 2D paw position) exceeded $V_{ORT_{x,y}}$ (Wilcoxon matched-pairs test, $Z = 2.02$, $n = 5$, $P < 0.05$) in those phases of swing in which $\Delta V_{x,y}$ was positive (Fig. 7). ANOVA performed on z-transformed V_{UCM} values revealed significant effect of swing time ($F_{9,36} = 6.48$, $P < 0.05$), time-limb interaction ($F_{9,36} = 2.7$, $P < 0.05$), and no significant effect of limb or walking condition. V_{ORT} was significantly affected by swing time ($F_{9,36} = 19.9$, $P < 0.05$) and by time-limb ($P < 0.05$, $F_{9,36} = 5.25$) and time-task ($P < 0.05$, $F_{9,36} = 2.63$)

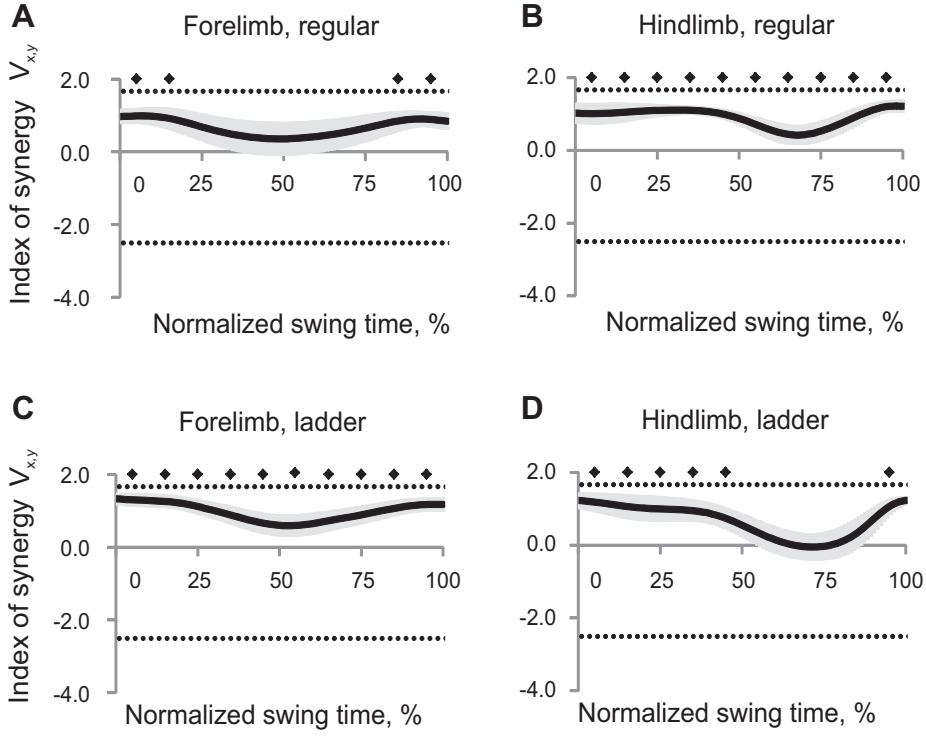

Fig. 5. Index of synergy $\Delta V_{x,y}$ as a function of the normalized swing time [mean (black line) ± SE (gray shadow), 5 cats] computed for the 2D paw position in space of 5 elemental variables. *A*: forelimb, regular walking. *B*: hindlimb, regular walking. *C*: forelimb, ladder walking. *D*: hindlimb, ladder walking. The *top* horizontal dotted line indicates the theoretical maximum of $\Delta V_{x,y}$ (1.67); the *bottom* dotted line indicates the theoretical minimum of $\Delta V_{x,y}$ (−2.5, see text for details). Solid diamonds indicate 10% time bins of swing for which $\Delta V_{x,y}$ is significantly different from zero ($P < 0.05$).

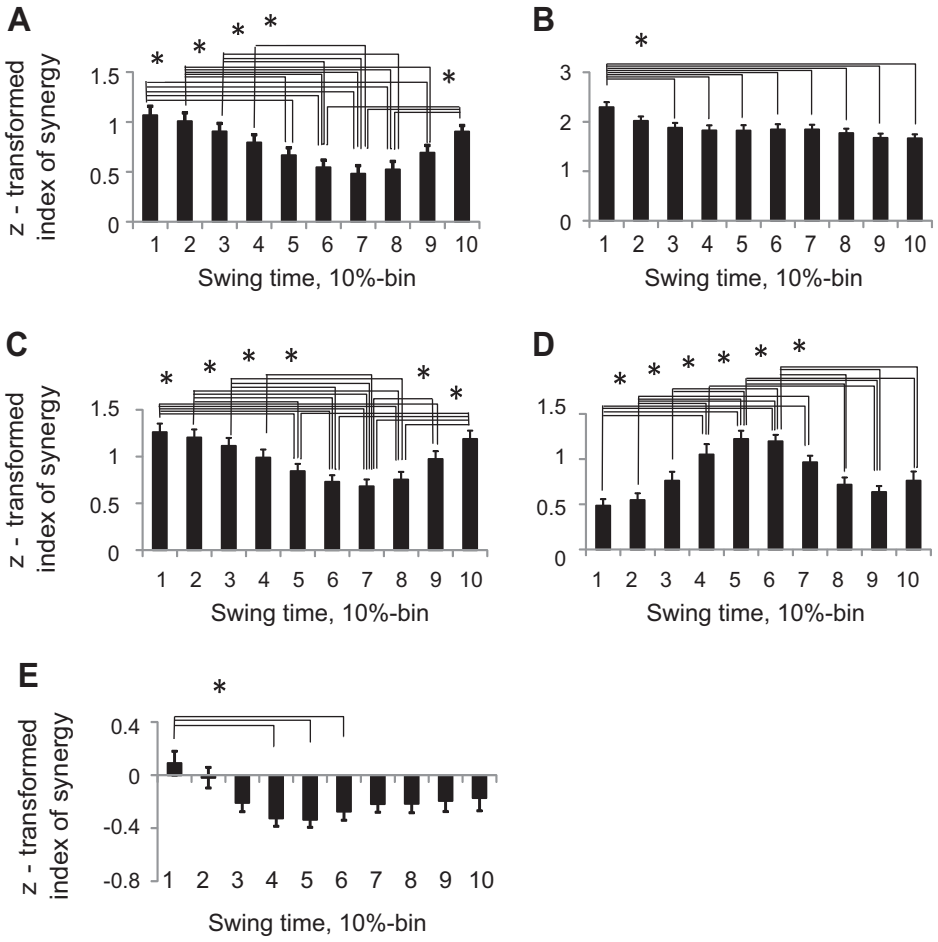

Fig. 6. *Z*-transformed index of synergy values averaged across limbs and walking conditions for each swing time bin (mean ± SE, 5 cats). *A*: index of synergy $\Delta V_{x,y}$. *B*: index of synergy ΔV_y. *C*: index of synergy ΔV_x. *D*: index of synergy ΔV_L. *E*: index of synergy ΔV_θ. Asterisks and horizontal brackets indicate statistical difference between time bins ($P < 0.05$).

interactions. The limb-task interaction effect was not significant ($P = 0.05$, $F_{1,4} = 7.68$).

Paw vertical position in 5D space of elemental variables. Mean synergy index ΔV_y computed across all cats for each task and limb had positive values (Wilcoxon matched-pairs test, $Z = 2.02$, $n = 5$, $P < 0.05$), approaching the theoretical maximum 1.25 throughout the entire swing for both limbs and walking tasks, except for hindlimb during midswing of ladder walking (Fig. 8). Thus forepaw and hindpaw vertical position was highly stabilized during swing phase of regular and ladder walking, whereas hindpaw vertical position was not stabilized in midswing (30–50% of swing time) of ladder walking. ANOVA performed on *z*-transformed ΔV_y values demonstrated a significant effect of swing time ($F_{9,36} = 6.45$, $P < 0.05$); the index of synergy ΔV_y averaged across limbs and walking conditions for each time bin was higher in early swing (10%) than later in swing (30–100% of swing time, Fig. 6*B*). Locomotion task also significantly affected ΔV_y ($F_{1,4} = 12.2$; $P < 0.05$), as the synergy index during regular walking was higher than during ladder walking. There were also significant time-limb ($F_{9,36} = 15.1$; $P < 0.05$) and time-task ($F_{9,36} = 3.55$; $P < 0.05$) interaction effects on ΔV_y.

Patterns of V_{UCM} for the vertical paw position (Fig. 9) were generally similar to those of the 2D paw position (Fig. 7), which was not the case for V_{ORT_y} values (Fig. 9) that were close to zero throughout most of swing, except for midswing of hindpaw during ladder walking.

Paw horizontal position in 5D space of elemental variables. Values of synergy index ΔV_x were positive (horizontal paw position was stabilized) in early and late swing of ladder walking for both fore- and hindpaw; they were also positive in mid- and late swing of hindpaw during regular walking (Wilcoxon matched-pairs test, $Z = 2.02$, $n = 5$, $P < 0.05$, Fig. 10). Synergy index was not different from zero during the entire swing for forepaw of regular walking. *Z*-transformed ΔV_x values were significantly affected by swing time (ANOVA, $F_{9,36} = 14.88$, $P < 0.05$); the index of synergy ΔV_x averaged across limbs and walking conditions for each time bin was higher in early (0–40%) and late swing (80–100%) than in midswing (50–70%, Fig. 6*C*). There was a significant time-limb interaction ($F_{9,36} = 8.54$; $P < 0.05$) and time-task interaction effect ($F_{9,36} = 2.49$; $P < 0.05$) on index of synergy ΔV_x, and no significant effects of locomotion task or limb. Patterns of V_{UCM_x} and V_{ORT_x} were generally similar to those determined for the 2D paw position with generally higher values of V_{ORT_x} (not shown).

Limb length in 3D space of elemental variables. Length of forelimb and hindlimb was stabilized during midswing of regular and ladder walking as index of synergy was positive (Wilcoxon matched-pairs test, $Z = 2.02$, $n = 5$, $P < 0.05$) and close to the maximum value 1.5 (Fig. 11). Forelimb length was also stabilized in late swing of regular and ladder walking. ANOVA performed on *z*-transformed ΔV_L values showed that limb length stabilization was significantly affected by swing

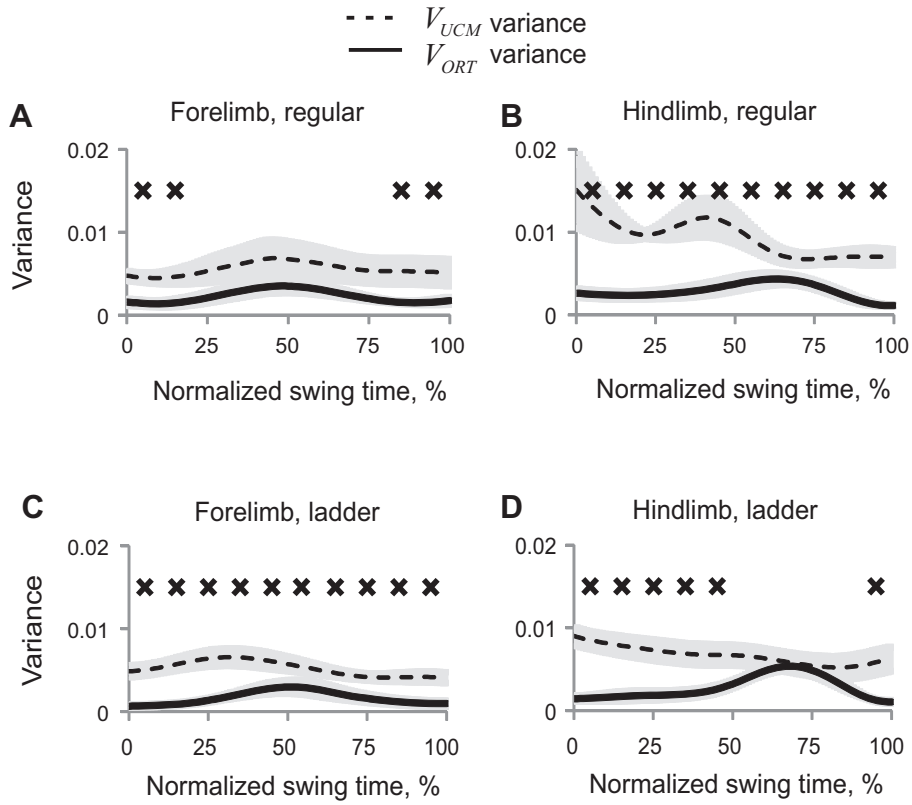

Fig. 7. Patterns of good (V_{UCM}, dashed line) and bad variance (V_{ORT}, solid line) (mean ± SE, 5 cats) computed for the 2D paw position in space of 5 elemental variables. *A*: forelimb, regular walking. *B*: hindlimb, regular walking. *C*: forelimb, ladder walking. *D*: hindlimb, ladder walking. X's indicate 10% time bins of swing for which V_{UCM} is significantly greater than V_{ORT} ($P < 0.05$).

time ($F_{9,36} = 12.74$, $P < 0.05$, Fig. 6*D*); the index of synergy ΔV_L averaged across limbs and walking conditions for each time bin was higher in midswing (time *bins 5* and *6*) than in early or late swing. Limb also had a significant effect on index of synergy ($F_{1,4} = 34.19$; $P < 0.05$): ΔV_L for forelimb was higher than for hindlimb. There was a significant time-limb interaction ($F_{9,36} = 4.57$; $P < 0.05$) and time-task interaction effects on index of synergy ΔV_L ($F_{9,36} = 4.79$; $P < 0.05$).

High levels of limb length stabilization in midswing resulted from elevated V_{UCM_L} variance during that phase of movement,

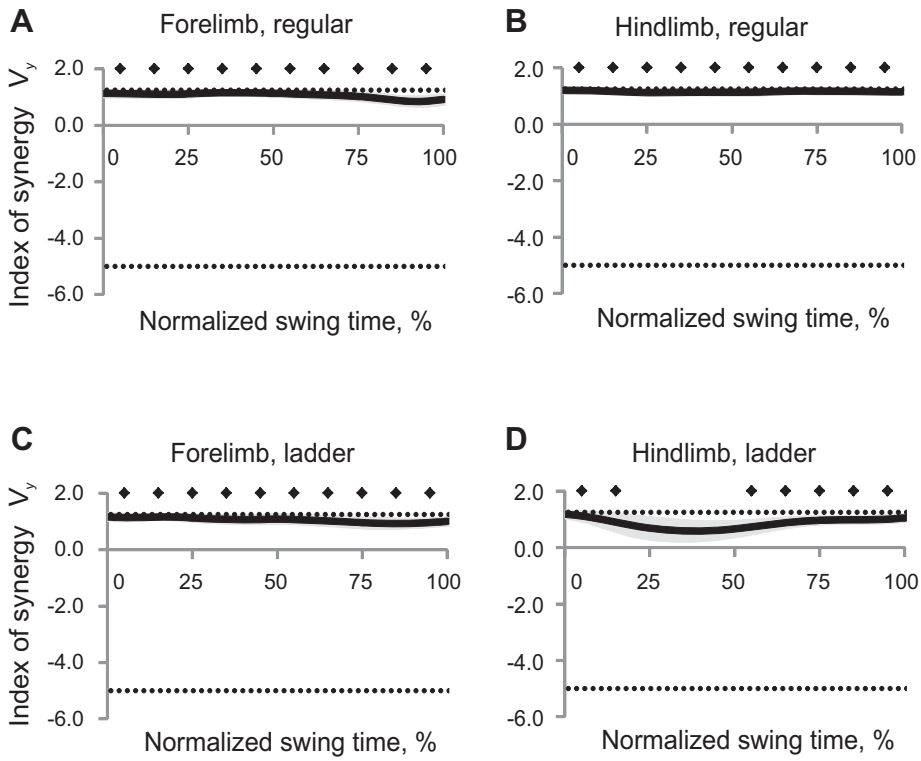

Fig. 8. Index of synergy ΔV_y as a function of the normalized swing time (mean ± SE, 5 cats) computed for the vertical paw position in space of 5 elemental variables. *A*: forelimb, regular walking. *B*: hindlimb, regular walking. *C*: forelimb, ladder walking. *D*: hindlimb, ladder walking. The *top* horizontal dotted line indicates the theoretical maximum of ΔV_y (1.25); the *bottom* dotted line indicates the theoretical minimum of ΔV_y (−5.0, see text for details). Solid diamonds indicate 10% time bins of swing for which ΔV_y is significantly different from zero ($P < 0.05$).

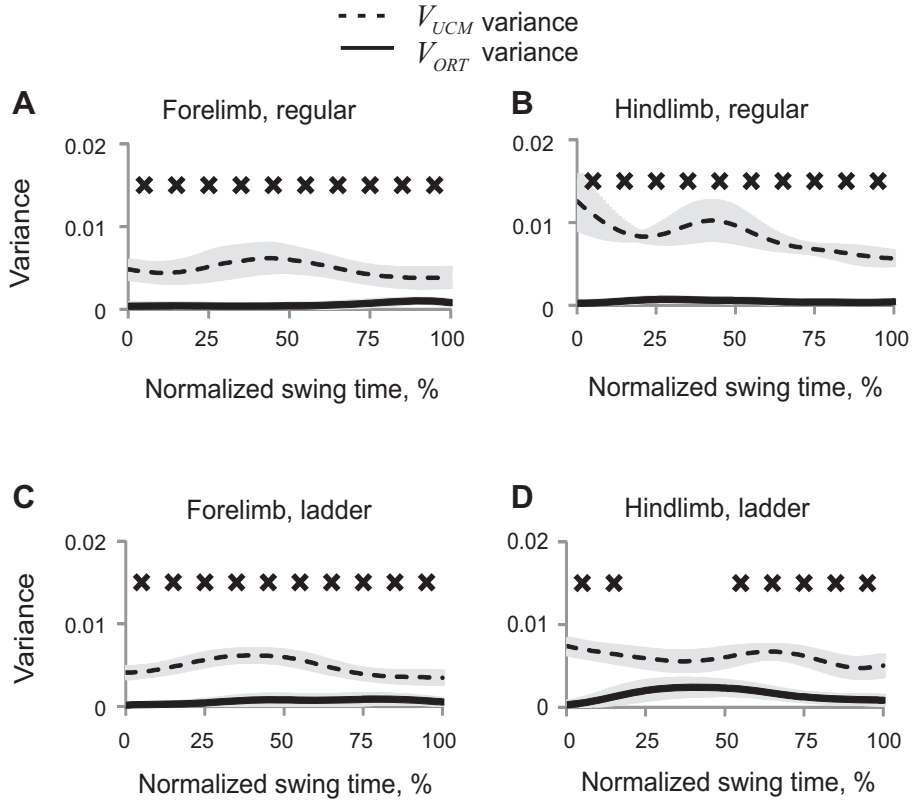

Fig. 9. Patterns of good (V_{UCM}, dashed line) and bad variance (V_{ORT}, solid line) (mean ± SE, 5 cats) computed for the vertical paw position in space of 5 elemental variables. *A*: forelimb, regular walking. *B*: hindlimb, regular walking. *C*: forelimb, ladder walking. *D*: hindlimb, ladder walking. X's indicate 10% time bins of swing for which V_{UCM} is significantly greater than V_{ORT} ($P < 0.05$).

while V_{ORT_L} values remained relatively constant throughout swing (Fig. 12).

Limb orientation in 3D space of elemental variables. Values of synergy index ΔV_θ computed for orientation of fore- and hindlimbs during regular and ladder walking were often negative (Wilcoxon matched-pairs test, $Z = 2.02$, $n = 5$, $P < 0.05$) except for short time periods in early swing (fore- and hindlimb during ladder walking) and late swing (forelimb during regular and ladder walking, Fig. 13). Negative synergy index indicates that leg orientation was not actively stabilized during most of swing. ANOVA performed on *z*-transformed ΔV_θ values demonstrated a significant effect of swing time ($F_{9,36} = 3.43$, $P < 0.05$, Fig. 6*E*); the index of synergy ΔV_θ averaged across limbs and walking conditions for each time bin was higher at 10% of swing time than at 40–60% of swing phase (Fig. 6*E*). Although there was no significant effect of locomotor task or limb

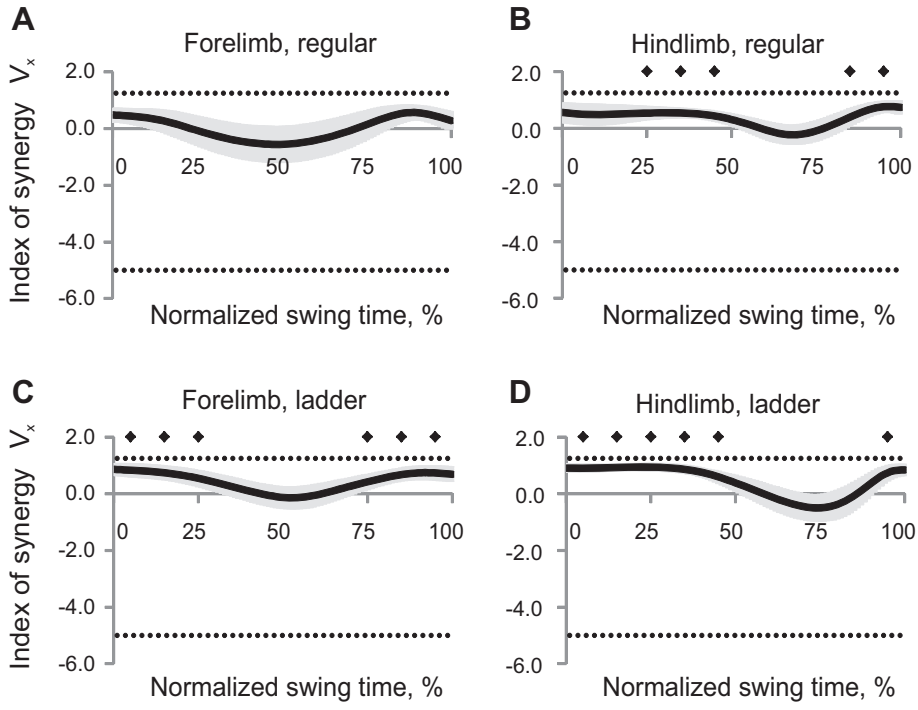

Fig. 10. Index of synergy ΔV_x as a function of the normalized swing time (mean ± SE, 5 cats) computed for the horizontal paw position in space of 5 elemental variables. *A*: forelimb, regular walking. *B*: hindlimb, regular walking. *C*: forelimb, ladder walking. *D*: hindlimb, ladder walking. The *top* horizontal dotted line indicates the theoretical maximum of ΔV_x (1.25); the *bottom* dotted line indicates the theoretical minimum of ΔV_x (−5.0, see text for details). Solid diamonds indicate 10% time bins of swing for which ΔV_x is significantly different from zero ($P < 0.05$).

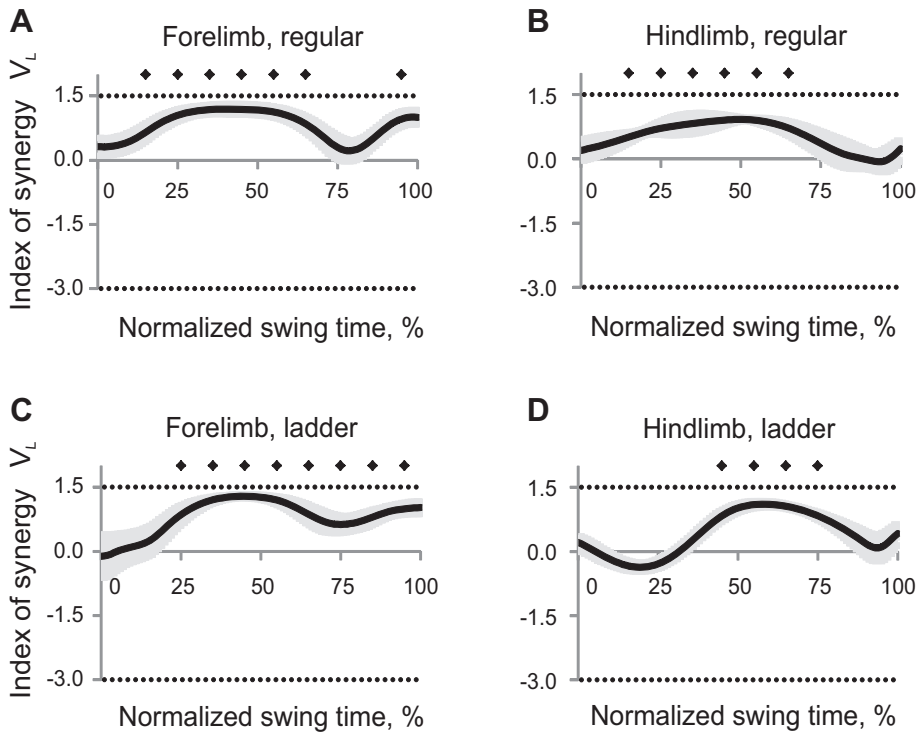

Fig. 11. Index of synergy ΔV_L as a function of the normalized swing time (mean ± SE, 5 cats) computed for the limb length in space of 3 elemental variables. *A*: forelimb, regular walking. *B*: hindlimb, regular walking. *C*: forelimb, ladder walking. *D*: hindlimb, ladder walking. The *top* horizontal dotted line indicates the theoretical maximum of ΔV_L (1. 5); the *bottom* dotted line indicates the theoretical minimum of ΔV_L (−3.0, see text for details). Solid diamonds indicate 10% time bins of swing for which ΔV_L is significantly different from zero ($P < 0.05$).

on ΔV_θ, there was significant time-limb interaction ($F_{9,36} = 5.5$; $P < 0.05$) and time-task interaction effects ($F_{9,36} = 5.9$; $P < 0.05$) on index of synergy ΔV_θ.

Large negative values of synergy index ΔV_θ during mid-swing of regular and ladder walking for both forelimbs and hindlimbs resulted from the peak of V_{ORT_θ} variance in mid-swing, while V_{UCM_θ} was not changing substantially during swing (Fig. 14).

DISCUSSION

This study is the first to demonstrate that cats organize the kinematics of locomotion based on the principle of abundance:

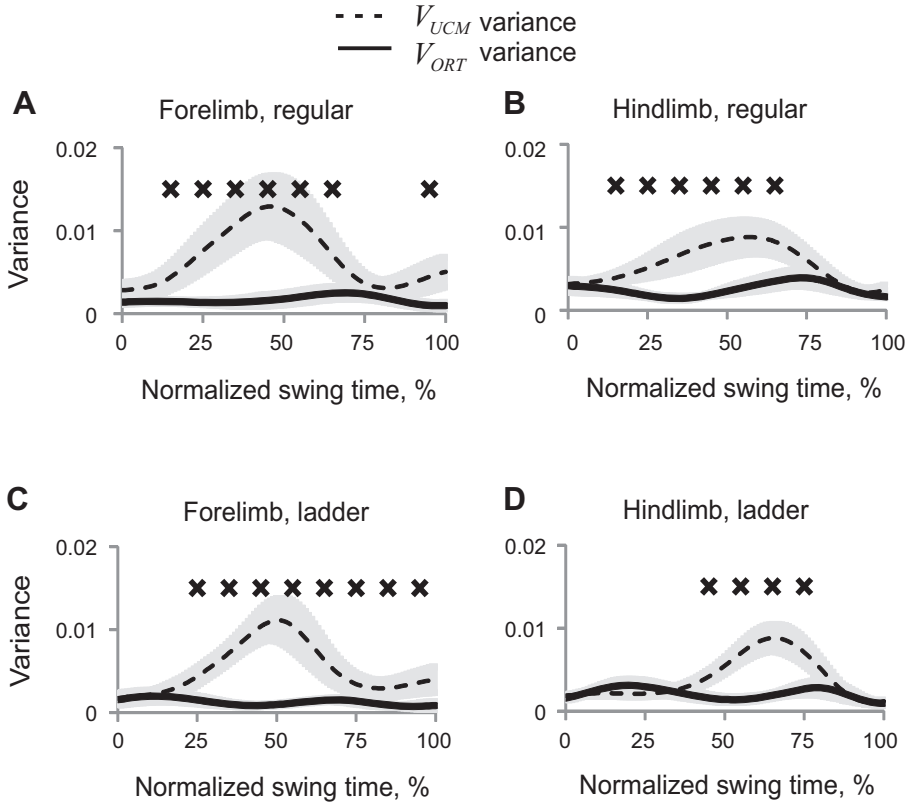

Fig. 12. Patterns of good (V_{UCM}, dashed line) and bad variance (V_{ORT}, solid line) (mean ± SE, 5 cats) computed for the limb length in space of 3 elemental variables. *A*: forelimb, regular walking. *B*: hindlimb, regular walking. *C*: forelimb, ladder walking. *D*: hindlimb, ladder walking. X's indicate 10% time bins of swing for which V_{UCM} is significantly greater than V_{ORT} ($P < 0.05$).

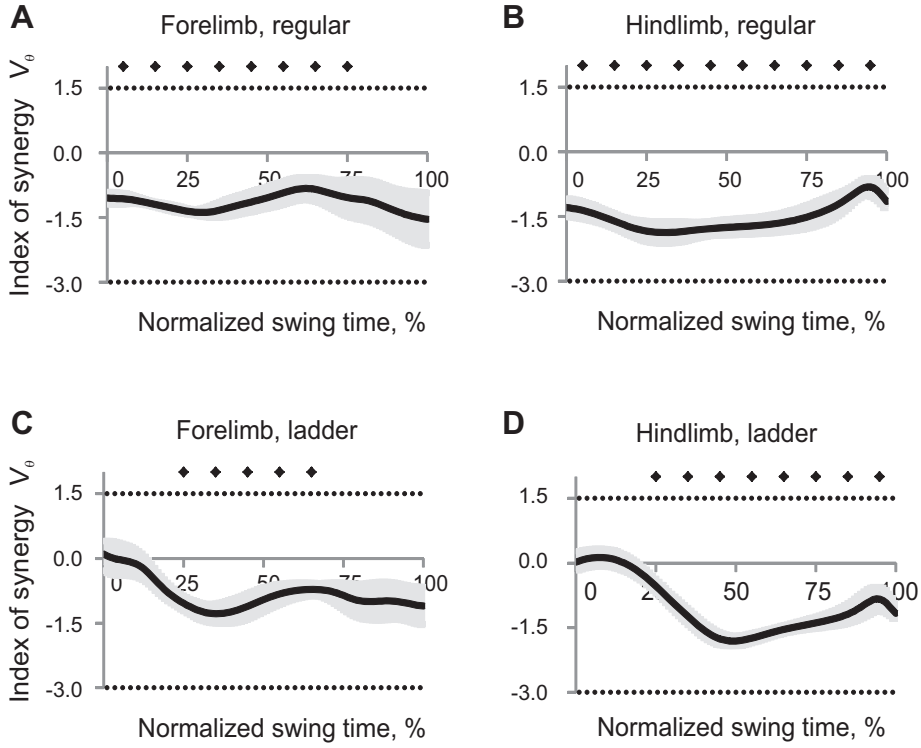

Fig. 13. Index of synergy ΔV_θ as a function of the normalized swing time (mean ± SE, 5 cats) computed for the limb orientation in space of 3 elemental variables. *A*: forelimb, regular walking. *B*: hindlimb, regular walking. *C*: forelimb, ladder walking. *D*: hindlimb, ladder walking. The *top* horizontal dotted line indicates the theoretical maximum of ΔV_θ (1. 5); the *bottom* dotted line indicates the theoretical minimum of ΔV_θ (−3.0, see text for details). Solid diamonds indicate 10% time bins of swing for which ΔV_θ is significantly different from zero ($P < 0.05$).

they use variable time profiles of elemental variables (limb generalized coordinates) to ensure relatively reproducible trajectory of several limb kinematic variables during the swing phase. The indexes of synergy $\Delta V_{x,y}$, ΔV_x, ΔV_y, ΔV_L, and ΔV_θ computed for each potential performance variable indicate that the vertical paw position was most consistently stabilized throughout the swing phase of regular and ladder walking for both fore- and hindpaw (Fig. 8). Since the horizontal paw position was also stabilized in initial and late swing of ladder walking and the horizontal hindpaw position was stabilized in

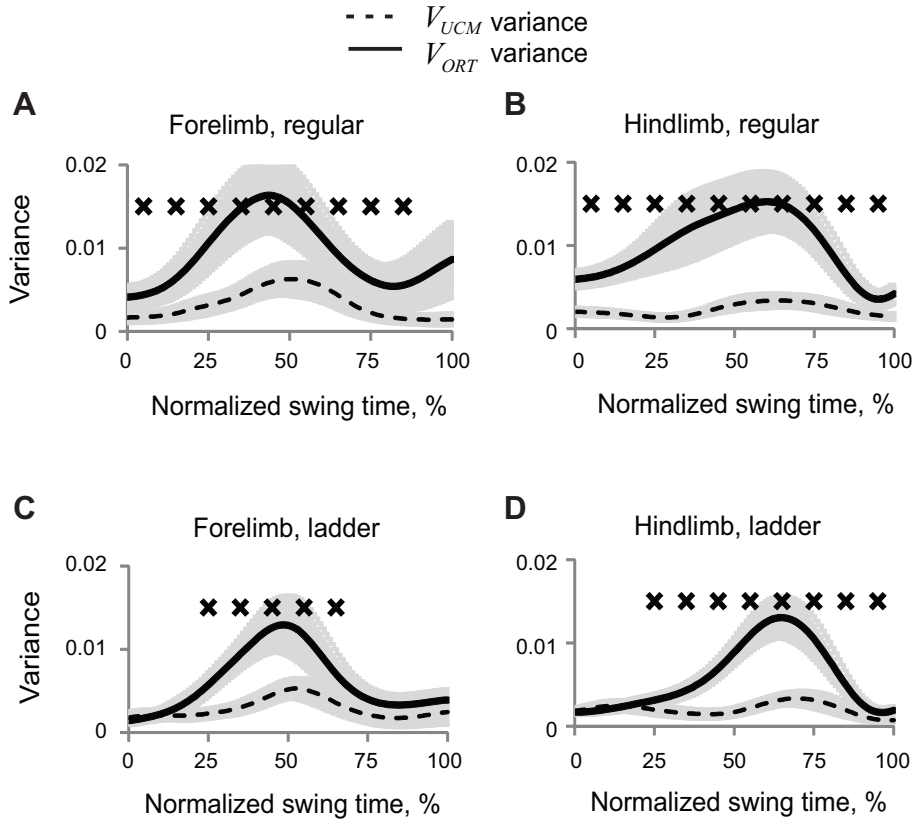

Fig. 14. Patterns of good (V_{UCM}, dashed line) and bad variance (V_{ORT}, solid line) (mean ± SE, 5 cats) computed for the limb orientation in space of 3 elemental variables. *A*: forelimb, regular walking. *B*: hindlimb, regular walking. *C*: forelimb, ladder walking. *D*: hindlimb, ladder walking. X's indicate 10% time bins of swing for which V_{UCM} is significantly smaller than V_{ORT} ($P < 0.05$).

late and midswing of regular walking (Fig. 10), it can be concluded that cats stabilized 2D paw position most consistently in early and late swing (see also Fig. 5 and Fig. 6, *A* and *C*). Furthermore, length of fore- and hindlimb was stabilized (in intrinsic, body-centered rather than in extrinsic, world-centered coordinates) in midswing of both walking tasks (Figs. 6*D* and 11). The limb length stabilization in midswing appears to occur at the expense of greater V_{ORT_θ} variability of limb orientation (Figs. 6, *D* and *E*, 12, and 14). Taken together, the above results suggest that the nervous system might stabilize different sets of performance variables at different movement phases.

None of the three hypotheses formulated in the Introduction received unambiguous support for the three identified performance variables: 2D paw position, vertical paw position and limb length. Indeed, while the cats stabilized the vertical paw trajectory (*hypothesis 1*), they did so for the entire swing phase only in three out of four studied combinations of limbs and walking conditions; hindpaw vertical position during ladder walking was stabilized only over the early and late phases of swing, not during the midswing. Similar conclusions could be drawn about stabilization of 2D paw position that occurred in early and late swing in three out of four limb-walking task combinations, and about limb length stabilization observed in midswing. Since synergy index ΔV_y during regular walking exceeded that during ladder walking, *hypothesis 2* was not supported for vertical paw position, although it was supported for 2D paw position and limb length. Finally, *hypothesis 3* was supported for limb length stabilization because ΔV_L for forelimb was higher than for hindlimb; however, *hypothesis 3* was not supported for 2D and vertical paw positions.

There are two major views on the problem of motor redundancy. One of them follows the classical formulation of Bernstein (1967) that the CNS "eliminates redundant degrees-of-freedom"; it assumes that single solutions are generated by the CNS, possibly based on an optimization principle (reviewed in Prilutsky and Zatsiorsky 2002; Seif-Naraghi and Winters 1990). The alternative view is that no DOF are ever eliminated, but they are all used in a covarying fashion to ensure stable performance with respect to important variables (principle of abundance, reviewed in Latash 2012). The UCM hypothesis has been developed based on the idea of abundance (Scholz and Schoner 1999) and applied to a variety of levels of analysis and tasks performed by different human populations (reviewed in Latash et al. 2007). The present study is the first one to show that the principle of abundance is not specific to human motor control, and that the method of UCM analysis can be successfully used to analyze movements of other animals. Animal models in combination with UCM analysis permit now the mechanistic studies of neural structures responsible for organizing motor synergies.

Several studies applied the method of analysis of joint covariation to whole body kinematics during human cyclic actions, such as rhythmic swaying (Freitas et al. 2006) and locomotion (Krishnan et al. 2013; Verrel et al. 2010). In particular, the latter two studies documented multijoint coordination stabilizing features of the step parameters and foot trajectory over the swing cycle.

The control of paw 2D position prior to paw placement during walking may be expected, given that cats [according to preliminary results (Rivers et al. 2010)] and humans (Patla and Vickers 2003) fix gaze at an intended stepping location two strides (in cats) or one stride (in humans) ahead of forepaw/foot placement. In addition, humans use the lower visual field to monitor foot trajectory during late swing of walking and use this information to improve accuracy of visually guided stepping (Marigold and Patla 2008; Reynolds and Day 2005). During accurate stepping, cats shift and rotate the head closer to the ground, presumably for a better view of the intended paw placement position (Beloozerova et al. 2010). Ensuring low variability of the paw 2D coordinates immediately prior to ground contact could also be expected because accurate paw placement is necessary for dynamically stable locomotion. Walking can be considered dynamically unstable if the vertical projection of the extrapolated center of mass of the body (that incorporates center of mass position and velocity) is beyond the base of support (Hof et al. 2005). To recover balance in this situation, the foot must be placed in front of the extrapolated center of mass and "in order to walk stable and in a straight path, the foot ... has to be placed with an accuracy of a few millimetres" (p. 257: Hof et al. 2007). A recent study on dynamic stability in walking cats (Farrell et al. 2011, 2014) indicates that the cat is dynamically unstable in the sagittal plane (the extrapolated center of mass is in front of the base of support) during the short phases of double support by diagonal fore- and hindlimbs. The forward fall of the cat is prevented by placement of the swing forepaw in front of the extrapolated center of mass during both regular walking and walking with a constrained stance width (Farrell et al. 2011, 2014). Hindpaw accurate placement in front of the extrapolated center of mass in the frontal plane may also be important for maintaining body lateral stability at the transition from a double support period by ipsilateral fore- and hindlimbs to a three-legged support period (Farrell et al. 2014). Thus covarying limb segment angles (and possibly other elemental variables) to ensure reproducible paw position prior to paw placement seems important not only for accurate stepping, but also for regular walking.

The need to stabilize paw position during the first half of swing is less intuitive, especially because paw horizontal position is stabilized much less for hindlimb during regular walking (Fig. 10) or not at all (forelimb during regular walking, Fig. 10). This result can be explained by *1*) considering that paw placement location is planned prior to swing onset (Hollands and Marple-Horvat 2001; 1996; Patla and Vickers 2003); and *2*) assuming that accuracy of paw preplanned stepping depends to a large extent on accurate estimation of paw initial position, which is not under direct visual control for either fore- or hindlimb in early swing.

More vigorous stabilization of 2D paw position in final swing stages may be needed to adjust paw position prior to ground contact since the paw placement location estimated prior to swing initiation may be outdated. Feedback corrections of paw trajectory seem more useful in late swing than in midswing if no major motion perturbation or obstacle appearance is expected. In such a situation, humans start correcting foot trajectory for accurate target stepping in the last 120 ms of the swing phase (Reynolds and Day 2005), the period consistent with the reaction time to simple visual stimuli. In cats this type of reaction time is faster, 60–70 ms (Pettersson 1990), given shorter distances for propagation of neural signals. With reaction time of 65 ms, paw trajectory corrections would be

expected to start at about 75–80% of swing time because, in our experiments, the swing durations were between 247 and 285 ms (Table 3). The obtained high positive values of the index of synergy $\Delta V_{x,y}$ for 2D paw position in late swing agree with these estimates (see Fig. 5).

A recent study of kinematic synergies stabilizing the foot trajectory during human locomotion has produced a different time profile of the synergy index: the index showed a peak in midswing and dropped close to the toe-off and heel-strike phases (Krishnan et al. 2013). While there are major differences in the design of the two studies, given that only a handful of studies applied the UCM-based method for analysis of kinematic synergies, comparing the results is warranted. In particular, the Krishnan et al. study analyzed synergy indexes with respect to the mediolateral foot trajectory only, while our study explored the paw trajectory in two dimensions in the sagittal plane. In addition, the bipedal walking of humans is associated with higher demands for stability and a higher ability to rely on vision for guiding foot placement during stepping, in particular compared with motion of the hindlimbs in cats. Also, the differences in the synergy indexes may reflect different ecological values of accurate stepping in cats and humans. While cats frequently navigate complex terrains with highly constrained support surfaces, modern humans typically walk in conditions where accurate foot placement is not crucial. In contrast, in midswing, high stabilization of the mediolateral foot trajectory in humans may reflect the desire to avoid collision with the supporting leg.

One of the identified performance variables in this study, the limb length, was also stabilized mostly in midswing (Fig. 11). This stabilization could be related to the requirement of safe paw-ground clearance during midswing. High level of stabilization of vertical paw position throughout swing (Fig. 8) could contribute to both limb length stabilization in midswing and 2D paw position stabilization in early and late swing.

ANOVA revealed significantly higher index of synergy ΔV_y during regular walking than during ladder walking, whereas ΔV_L was found to be greater for forelimb than hindlimb. It has been demonstrated that, although forelimb kinematics during regular and skilled ladder walking are virtually identical (Beloozerova et al. 2010), the neural control mechanisms of these tasks are likely different. Regular walking can be performed without visual feedback (Beloozerova and Sirota 1993a), after lesion of motor cortex (Beloozerova and Sirota 1993a; Liddell and Phillips 1944) and in decerebrate (Shik et al. 1966) and spinal (Rossignol 2006) cats, whereas walking on a horizontal ladder is impossible in those conditions. Also, the modulation of neuronal activity from forelimb and hindlimb representations in the motor cortex is typically much higher during ladder walking (Armstrong and Marple-Horvat 1996; Beloozerova et al. 2010; Beloozerova and Sirota 1993a, 1993b; Drew et al. 2008). These data suggest that successful accurate stepping by the forelimbs requires visual input, which is integrated with motor cortical output. Thus different neural mechanisms involved in control of fore- and hindlimb movements during regular walking and accurate stepping appear to have differential effects on stabilization of paw position and limb length in several parts of the swing phase. The neural mechanisms responsible for hindpaw position stabilization may involve the asymmetric coupling between fore- and hindlimb locomotor pattern-generating networks (Juvin et al. 2012) and entrainment of hindlimb muscle activity by forelimbs during walking (Akay et al. 2006), also shown during postural corrections (Deliagina et al. 2006).

The combination of the nearly identical kinematics (Beloozerova et al. 2010) and modulation of indexes of synergy values (ΔV_y, $\Delta V_{x,y}$, ΔV_L, the present study) for the fore- and hindlimb swing trajectories during regular and ladder stepping (Figs. 5, 8, 11) fit the scheme of the control of redundant systems that assumes the presence of two major groups of variables (Latash 2010; Latash et al. 2005). One of them defines the time evolution of important task-specific performance variables, likely by generating neural signals that translate into trajectories of referent values for those variables. The other defines stability properties of those variables. Several studies of both kinematic and kinetic variables in humans have shown that the same performance can be associated with significantly different indexes of covariation among elemental variables (Freitas and Scholz 2009; Klous et al. 2011; Olafsdottir et al. 2005). Our present study shows that the ability of the CNS to modulate stability properties without changing the overall movement pattern is also present during cat locomotion.

Finally, it is important to note that the revealed high stabilization of three performance variables during fore- and hindlimb swing, 2D paw position, vertical paw position and limb length, is caused by different contributions of V_{UCM} and V_{ORT}. For example, high stabilization of paw 2D position in early and late swing was caused by the low V_{ORT} rather than high V_{UCM} (cf., Figs. 5 and 7), largest positive values of index of synergy $\Delta V_{x,y}$ occur in phases similar to those in which V_{ORT} had the smallest values. This observation suggests that neural commands responsible for strong stabilization of paw trajectories during specific phases of swing tend to reduce deviations of limb segment configurations that affect paw position instead of increasing variability of segment angles that does not influence paw trajectory. This strategy seems to promote less variable, more stereotypic joint angle patterns in locomotion phases where stabilization of swing paw position is important. On the other hand, high values of index of synergy for limb length ΔV_L in midswing (Fig. 11) resulted from increased V_{UCM} and small changes in V_{ORT} (Fig. 12), indicating the opposite strategy of stabilization of this performance variable. Note that human experiments have provided evidence for increased V_{UCM} during movements to uncertain targets and practice in conditions of instability (de Freitas et al. 2007; Freitas and Scholz 2009; Wu et al. 2012). The differences in patterns of V_{UCM} and V_{ORT} for endpoint limb position between human movements and cat walking could reflect relatively high dynamic stability of quadrupedal locomotion (Farrell et al. 2011; Farrell et al. 2014).

In conclusion, we would like to acknowledge certain shortcomings of the present study. The first, and most obvious, one is the small number of animals that could potentially preclude us from reaching significance in some statistical tests. We would like to mention, however, that a large number of tests, in particular those directly related to testing the specific hypotheses, did lead to significant results. Hence, we can conclude that the sample sizes in our comparisons were sufficiently large. Second, we analyzed only a subset of kinematic variables potentially important for locomotion. For example, trajectory of the center of mass was not analyzed as a potential

variable stabilized by multijoint synergies. This is partly due to problems in building a kinematic model that would link center of mass velocity to joint velocities, given that the center of mass location within the body migrates during locomotion and the spine kinematics cannot be easily reduced to a few fixed joint rotations. Third, it is possible that, due to temporal variability across strides, comparability of limb postures at specific time instances of swing could be compromised, particularly in midswing, when joint velocities are relatively high. This could have potentially had an impact on our analyses by adding spatial variance related to imprecise time alignment across strides. These effects, however, were likely small, because the temporal variability of elemental and potential performance variables was low (Figs. 2 and 3). Fourth, we used only one method of assessment of multijoint synergies. Other methods (for example, Muller and Sternad 2003; Verrel 2011; Yen and Chang 2010) could provide complementary information on the control of the kinematics of cat locomotion.

ACKNOWLEDGMENTS

Authors are indebted to Erik E. Stout, Dr. Mikhail G. Sirota and Dr. Guay-haur Shue for help with data collection and technical assistance.

Present address of B. J. Farrell: Hulse Spinal Cord Injury Lab, Shepherd Center, 2020 Peachtree Rd. NW, Atlanta, GA 30309-1465.

GRANTS

This work was partly supported by National Institutes of Health Grants HD-32571 and EB-012855 (to B. I. Prilutsky) and NS-058659 (to I. N. Beloozerova), and the Center for Human Movement Studies at Georgia Tech.

DISCLOSURES

No conflicts of interest, financial or otherwise, are declared by the author(s).

AUTHOR CONTRIBUTIONS

Author contributions: A.N.K., B.J.F., I.N.B., and B.I.P. performed experiments; A.N.K. and B.J.F. analyzed data; A.N.K., I.N.B., M.L.L., and B.I.P. interpreted results of experiments; A.N.K. prepared figures; A.N.K. and B.I.P. drafted manuscript; A.N.K., B.J.F., I.N.B., M.L.L., and B.I.P. approved final version of manuscript; B.J.F., I.N.B., M.L.L., and B.I.P. edited and revised manuscript; I.N.B., M.L.L., and B.I.P. conception and design of research.

REFERENCES

Akay T, McVea DA, Tachibana A, Pearson KG. Coordination of fore and hind leg stepping in cats on a transversely-split treadmill. *Exp Brain Res* 175: 211–222, 2006.

Armstrong DM, Marple-Horvat DE. Role of the cerebellum and motor cortex in the regulation of visually controlled locomotion. *Can J Physiol Pharmacol* 74: 443–455, 1996.

Auyang AG, Yen JT, Chang YH. Neuromechanical stabilization of leg length and orientation through interjoint compensation during human hopping. *Exp Brain Res* 192: 253–264, 2009.

Bauman JM, Chang YH. Rules to limp by: joint compensation conserves limb function after peripheral nerve injury. *Biol Lett* 9: 20130484, 2013.

Beloozerova IN, Farrell BJ, Sirota MG, Prilutsky BI. Differences in movement mechanics, electromyographic, and motor cortex activity between accurate and nonaccurate stepping. *J Neurophysiol* 103: 2285–2300, 2010.

Beloozerova IN, Sirota MG. The role of the motor cortex in the control of accuracy of locomotor movements in the cat. *J Physiol* 461: 1–25, 1993a.

Beloozerova IN, Sirota MG. The role of the motor cortex in the control of vigour of locomotor movements in the cat. *J Physiol* 461: 27–46, 1993b.

Berkinblit MB, Feldman AG, Fukson OI. Adaptability of innate motor patterns and motor control mechanisms. *Behav Brain Sci* 9: 585–638, 1986.

Bernstein NA. *The Co-ordination and Regulation of Movements*. Oxford, UK: Pergamon, 1967.

Bernstein NA. [Studies on biomechanics of hitting using optical recordings]. *Ann Central Institute Labor* 1: 19–79, 1923.

Bobath B. *Adult Hemiplegia: Evaluation and Treatment*. London: Heinemann, 1978.

Bosco G, Poppele RE, Eian J. Reference frames for spinal proprioception: limb endpoint based or joint-level based? *J Neurophysiol* 83: 2931–2945, 2000.

Boyce VS, Lemay MA. Modularity of endpoint force patterns evoked using intraspinal microstimulation in treadmill trained and/or neurotrophin-treated chronic spinal cats. *J Neurophysiol* 101: 1309–1320, 2009.

Chang YH, Auyang AG, Scholz JP, Nichols TR. Whole limb kinematics are preferentially conserved over individual joint kinematics after peripheral nerve injury. *J Exp Biol* 212: 3511–3521, 2009.

de Freitas SM, Scholz JP, Stehman AJ. Effect of motor planning on use of motor abundance. *Neurosci Lett* 417: 66–71, 2007.

Deliagina TG, Sirota MG, Zelenin PV, Orlovsky GN, Beloozerova IN. Interlimb postural coordination in the standing cat. *J Physiol* 573: 211–224, 2006.

Dewald JP, Pope PS, Given JD, Buchanan TS, Rymer WZ. Abnormal muscle coactivation patterns during isometric torque generation at the elbow and shoulder in hemiparetic subjects. *Brain* 118: 495–510, 1995.

Dingwell JB, Robb RT, Troy KL, Grabiner MD. Effects of an attention demanding task on dynamic stability during treadmill walking. *J Neuroeng Rehabil* 5: 12, 2008.

Domkin D, Laczko J, Djupsjobacka M, Jaric S, Latash ML. Joint angle variability in 3D bimanual pointing: uncontrolled manifold analysis. *Exp Brain Res* 163: 44–57, 2005.

Drew T, Andujar JE, Lajoie K, Yakovenko S. Cortical mechanisms involved in visuomotor coordination during precision walking. *Brain Res Rev* 57: 199–211, 2008.

Farrell BJ, Bulgakova M, Sirota MG, Prilutsky BI, Beloozerova IN. Frontal plane mechanics and activity of motor cortex during locomotion tasks with challenging requirements for lateral stability. Program No. 710.710. In: *2011 Neuroscience Meeting Planner*. Washington, DC: Society for Neuroscience 2011.

Farrell BJ, Bulgakova MA, Beloozerova IN, Sirota MG, Prilutsky BI. Body stability and muscle and motor cortex activity during walking with wide stance. *J Neurophysiol*. In press, 2014.

Freitas SM, Duarte M, Latash ML. Two kinematic synergies in voluntary whole-body movements during standing. *J Neurophysiol* 95: 636–645, 2006.

Freitas SM, Scholz JP. Does hand dominance affect the use of motor abundance when reaching to uncertain targets? *Hum Mov Sci* 28: 169–190, 2009.

Galvez-Lopez E, Maes LD, Abourachid A. The search for stability on narrow supports: an experimental study in cats and dogs. *Zoology (Jena)* 114: 224–232, 2011.

Gelfand IM, Latash ML. On the problem of adequate language in motor control. *Motor Control* 2: 306–313, 1998.

Goodman SR, Latash ML. Feed-forward control of a redundant motor system. *Biol Cybern* 95: 271–280, 2006.

Gorniak SL, Duarte M, Latash ML. Do synergies improve accuracy? A study of speed-accuracy trade-offs during finger force production. *Motor Control* 12: 151–172, 2008.

Gregor RJ, Smith DW, Prilutsky BI. Mechanics of slope walking in the cat: quantification of muscle load, length change, and ankle extensor EMG patterns. *J Neurophysiol* 95: 1397–1409, 2006.

Hof AL, Gazendam MG, Sinke WE. The condition for dynamic stability. *J Biomech* 38: 1–8, 2005.

Hof AL, van Bockel RM, Schoppen T, Postema K. Control of lateral balance in walking. Experimental findings in normal subjects and above-knee amputees. *Gait Posture* 25: 250–258, 2007.

Hollands MA, Marple-Horvat DE. Coordination of eye and leg movements during visually guided stepping. *J Mot Behav* 33: 205–216, 2001.

Hollands MA, Marple-Horvat DE. Visually guided stepping under conditions of step cycle-related denial of visual information. *Exp Brain Res* 109: 343–356, 1996.

Hultborn H, Brownstone RB, Toth TI, Gossard JP. Key mechanisms for setting the input-output gain across the motoneuron pool. *Prog Brain Res* 143: 77–95, 2004.

Juvin L, Le Gal JP, Simmers J, Morin D. Cervicolumbar coordination in mammalian quadrupedal locomotion: role of spinal thoracic circuitry and limb sensory inputs. *J Neurosci* 32: 953–965, 2012.

Kapur S, Friedman J, Zatsiorsky VM, Latash ML. Finger interaction in a three-dimensional pressing task. *Exp Brain Res* 203: 101–118, 2010.

Klous M, Mikulic P, Latash ML. Two aspects of feedforward postural control: anticipatory postural adjustments and anticipatory synergy adjustments. *J Neurophysiol* 105: 2275–2288, 2011.

Krishnan V, Rosenblatt NJ, Latash ML, Grabiner MD. The effects of age on stabilization of the mediolateral trajectory of the swing foot. *Gait Posture* 38: 923–928, 2013.

Latash ML. The bliss (not the problem) of motor abundance (not redundancy). *Exp Brain Res* 217: 1–5, 2012.

Latash ML. Motor synergies and the equilibrium-point hypothesis. *Motor Control* 14: 294–322, 2010.

Latash ML, Scholz JP, Schoner G. Toward a new theory of motor synergies. *Motor Control* 11: 276–308, 2007.

Latash ML, Shim JK, Smilga AV, Zatsiorsky VM. A central back-coupling hypothesis on the organization of motor synergies: a physical metaphor and a neural model. *Biol Cybern* 92: 186–191, 2005.

Lavoie S, McFadyen B, Drew T. A kinematic and kinetic analysis of locomotion during voluntary gait modification in the cat. *Exp Brain Res* 106: 39–56, 1995.

Liddell EG, Phillips CG. Pyramidal section in the cat. *Brain* 67: 1–9, 1944.

MacLellan MJ, Patla AE. Adaptations of walking pattern on a compliant surface to regulate dynamic stability. *Exp Brain Res* 173: 521–530, 2006.

Marigold DS, Patla AE. Visual information from the lower visual field is important for walking across multi-surface terrain. *Exp Brain Res* 188: 23–31, 2008.

Martin V, Scholz JP, Schoner G. Redundancy, self-motion, and motor control. *Neural Comput* 21: 1371–1414, 2009.

McAndrew Young PM, Wilken JM, Dingwell JB. Dynamic margins of stability during human walking in destabilizing environments. *J Biomech* 45: 1053–1059, 2012.

Metz GA, Whishaw IQ. Cortical and subcortical lesions impair skilled walking in the ladder rung walking test: a new task to evaluate fore- and hindlimb stepping, placing, and co-ordination. *J Neurosci Methods* 115: 169–179, 2002.

Miller S, Van Der Burg J, Van Der Meche F. Coordination of movements of the hindlimbs and forelimbs in different forms of locomotion in normal and decerebrate cats. *Brain Res* 91: 217–237, 1975.

Muller H, Sternad D. A randomization method for the calculation of covariation in multiple nonlinear relations: illustrated with the example of goal-directed movements. *Biol Cybern* 89: 22–33, 2003.

Mussa-Ivaldi FA, Giszter SF, Bizzi E. Linear combinations of primitives in vertebrate motor control. *Proc Natl Acad Sci U S A* 91: 7534–7538, 1994.

Olafsdottir H, Yoshida N, Zatsiorsky VM, Latash ML. Anticipatory covariation of finger forces during self-paced and reaction time force production. *Neurosci Lett* 381: 92–96, 2005.

Pantall A, Gregor RJ, Prilutsky BI. Stance and swing phase detection during level and slope walking in the cat: effects of slope, injury, subject and kinematic detection method. *J Biomech* 45: 1529–1533, 2012.

Park J, Lewis MM, Huang X, Latash ML. Effects of olivo-ponto-cerebellar atrophy (OPCA) on finger interaction and coordination. *Clin Neurophysiol* 124: 991–998, 2013.

Park J, Wu YH, Lewis MM, Huang X, Latash ML. Changes in multifinger interaction and coordination in Parkinson's disease. *J Neurophysiol* 108: 915–924, 2012.

Patla AE, Greig M. Any way you look at it, successful obstacle negotiation needs visually guided on-line foot placement regulation during the approach phase. *Neurosci Lett* 397: 110–114, 2006.

Patla AE, Vickers JN. How far ahead do we look when required to step on specific locations in the travel path during locomotion? *Exp Brain Res* 148: 133–138, 2003.

Pettersson LG. Forelimb movements in the cat; kinetic features and neuronal control. *Acta Physiol Scand Suppl* 594: 1–60, 1990.

Prilutsky BI, Sirota MG, Gregor RJ, Beloozerova IN. Quantification of motor cortex activity and full-body biomechanics during unconstrained locomotion. *J Neurophysiol* 94: 2959–2969, 2005.

Prilutsky BI, Zatsiorsky VM. Optimization-based models of muscle coordination. *Exerc Sport Sci Rev* 30: 32–38, 2002.

Reisman DS, Scholz JP. Aspects of joint coordination are preserved during pointing in persons with post-stroke hemiparesis. *Brain* 126: 2510–2527, 2003.

Reynolds RF, Day BL. Visual guidance of the human foot during a step. *J Physiol* 569: 677–684, 2005.

Rivers TJ, Shaw NA, Sirota MG, Beloozerova IN. The relationship between vertical gaze shifts and stride cycle in freely walking cats. Program No. 278.273. In: *2010 Neuroscience Meeting Planner*. San Diego, CA: Society for Neuroscience, 2010.

Rossignol S. Plasticity of connections underlying locomotor recovery after central and/or peripheral lesions in the adult mammals. *Philos Trans R Soc Lond B Biol Sci* 361: 1647–1671, 2006.

Scholz JP, Schoner G. The uncontrolled manifold concept: identifying control variables for a functional task. *Exp Brain Res* 126: 289–306, 1999.

Scholz JP, Schoner G, Latash ML. Identifying the control structure of multijoint coordination during pistol shooting. *Exp Brain Res* 135: 382–404, 2000.

Seif-Naraghi AH, Winters JM. Optimized strategies for scaling goal-directed dynamic limb movements. In: *Multiple Muscle Systems Biomechanics and Movement Organization*, edited by Winters JM and Woo SL-Y. New York: Springer-Verlag, 1990, p. 312–334.

Shapkova EY, Shapkova AL, Goodman SR, Zatsiorsky VM, Latash ML. Do synergies decrease force variability? A study of single-finger and multi-finger force production. *Exp Brain Res* 188: 411–425, 2008.

Shik ML, Severin FV, Orlovskii GN. [Control of walking and running by means of electric stimulation of the midbrain]. *Biofizika* 11: 659–666, 1966.

Ting LH, McKay JL. Neuromechanics of muscle synergies for posture and movement. *Curr Opin Neurobiol* 17: 622–628, 2007.

Todorov E, Jordan MI. Optimal feedback control as a theory of motor coordination. *Nat Neurosci* 5: 1226–1235, 2002.

Verrel J. A formal and data-based comparison of measures of motor-equivalent covariation. *J Neurosci Methods* 200: 199–206, 2011.

Verrel J, Lovden M, Lindenberger U. Motor-equivalent covariation stabilizes step parameters and center of mass position during treadmill walking. *Exp Brain Res* 207: 13–26, 2010.

Wu YH, Pazin N, Zatsiorsky VM, Latash ML. Practicing elements vs. practicing coordination: changes in the structure of variance. *J Mot Behav* 44: 471–478, 2012.

Yang JF, Scholz JP. Learning a throwing task is associated with differential changes in the use of motor abundance. *Exp Brain Res* 163: 137–158, 2005.

Yen JT, Chang YH. Rate-dependent control strategies stabilize limb forces during human locomotion. *J R Soc Interface* 7: 801–810, 2010.